Master of Science Thesis

Development of Rotation-free Element for Membrane Wrinkled Analysis

by

Shankar Nagabhushana

Thesis submitted to the University of Wales in candidature for the degree of Master of Science

Supervisor: Dr. Antonio J Gil

Civil and Computational Engineering Centre
School of Engineering
Swansea University, Swansea
United Kingdom

June 2009

DECLARATION

This work has not previously been accepted in substance for any degree and is not being currently submitted in candidature for any degree.

Signed.....(candidate)
Date.....

STATEMENT 1

This thesis is the result of my own investigation, except where otherwise stated. Other sources are acknowledged by footnotes giving explicit references. A bibliography is appended.

Signed.....(candidate)
Date.....

STATEMENT 2

I hereby give consent for my thesis, if accepted, to be available for photocopying and for inter-library loan, and for the title and summary to be made available to outside organizations.

Signed.....(candidate)
Date.....

Summary

A Total Lagrangian formulation for prestressed structural membranes is described. The kinematics of prestressed membranes is displayed as a series of three successive configurations, namely, a nominally stressed initial equilibrium state, a prestressed state and a final in-service state, for the time instants t^0, t^{pret} and t, respectively. Kinematic entities are fully derived, i.e., deformations gradient tensor, displacement gradient tensor, right Cauchy-Green tensor or Green-Lagrange strain tensor.The Saint Venant-Kirchhoff model is chosen as hyperelastic materials to describe moderate strains behavior.

The equilibrium shapes are employed as initial guesses for the subsequent highly nonlinear problem that entails the structural analysis of the membrane with bending formulation under the actual presence of prestress loading and external loading.

A Total Lagrangian format set up along with a displacement-based isoparametric finite element formulation and a Newton-Raphson numerical scheme is adopted for the implementation of the Rotation Free Elements. Two-noded elements will be employed to describe appropriately cables and three-noded linear finite elements will be employed to describe membrane and Rotation free element.

For Rotation free element or Bending element formulation, a patch of the domain of the element is defined.Two triangular elements connecting an edge is taken as the patch, to derive the Kinematic entities.The $1/3^{rd}$ area of this two element is taken as the domain area for bending moment calculation. The curvature of the patch over the edge is approximated by central finite difference.The principal of virtual work is employed to get the equilibrium equation.The virtual work equation is linearized and discretized to get equivalent internal nodal force. For the implementation of the Newton-Rapson method, the internal nodal force is further linearized and discretized to get the total tangent stiffness matrix. The total tangent stiffness matrix has contribution due to nonlinear geometric and the constitutive part.Newton-Raphson numerical scheme is adopted for the implementation of the Rotation Free Elements. Through number of numerical examples the robustness and the validity of the formulation is shown.

Apart from the well known second order Newton-Raphson method, other first order procedures such as the steepest descent method, the Polak-Ribiere method or the Fletcher-Reeves method are employed. This results in a very flexible numerical solver.

Contents

List of Symbols and Abbreviations

Abbreviation	Description	Definition
A^{pret}	Prestress cable section area	
b	force field per unit mass	
$\mathbf{D}$	strain rate tensor	
e	Green-Lagrange strain vector	
$\mathbf{E}$	Green-Lagrange strain vector	
E	Young modulus	
$\mathbf{F}$	Deformation gradient tensor	
f	Equivalent external forces	
f	Deformation gradient tensor	
$\mathbf{G}$	Displacement gradient tensor	
$\mathbf{K}^{geo}$	Geometric Stiffness matrix	
$\mathbf{K}^{mat}$	Material stiffness matrix	
K^{geo}		
L^{pret}	prestressed cable length	
$\mathbf{M}^{geo}$	Geometric Stiffness matrix	
$\mathbf{M}^{mat}$	Material stiffness matrix	
N^I	Standard shape function	
$\mathbf{P}$	nominal stress tensor	
$\mathbf{R}$	Rotation tensor	
$\mathbf{s}$	Second Piola-Kirchhoff stress tensor	
$\mathbf{S}$	Second Piola-Kirchhoff stress tensor	
t	membrane thickness	
$\mathbf{u}$	nodal displacement	
$\mathbf{U}$	Stretch tensor	
V	Current Volume	
V^{pret}	Prestressed volume	
$\mathbf{x}$	Current coordinates	
$\mathbf{X}^{pret}$	Prestressed coordinates	
w_{int}	Helmholtz's free energy	
σ^{pret}	prestress Cauchy stress tensor	

Abbreviation	Description	Definition
σ	Cauchy stress tensor	
ν	Poisson ratio	
Γ^{pret}	Prestressed membrane area	
Π^{pret}	Total potential energy	
Π_{ext}	external potential energy	
$\delta\mathbf{u}$	virtual displacements	
U	internal potential energy	
ξ_{pret}	principal strains	
λ_α	principal stretches	
ρ^{pret}	prestressed density	
ρ	current density	

List of Figures

Acknowledgments

I would like to express my profound gratitude to Dr Antonio J Gil, for being my supervisor. He has been very helpful in guiding me and encouraging me to learn news things, without which, this thesis would not have been possible.

I would also like to thank Professor J Bonet for his guidance.

I am also thankful to European Commission for sponsoring this Erasmus Mundus Master Program and also to International Center for Numerical Methods in Engineering (CIMNE), Barcelona for forming such wonderful curriculum.

I would also like to thank Dr David Wakefield and all the staff at Tensys for their support for my internship.

I would like to thank all my friends in Swansea, specially Prabhu and Richard for all the discussion we had but never agreed to converge to a point. And also Sudharshan, Pavan, Chitra, Vinay and Ravi for making my stay at Swansea very memorable.

I would like to say special thanks to my brother and sisters. It would be worthwhile to mention each of them. Rajyashree, my sister for all her encouragement to perform at my best. Vedashree, my sister for all the methods, techniques to develop good concentration, confidence and fill my life with energy. Ravi Krishna, my brother for always supporting me in all my decisions and helping me fully concentrate on my studies. And finally to my aunt Nagavenamma, Nagalamba and my mother Vijayalaksmhi for their support, encouragement, blessing and specially their love.

Chapter 1

Preliminaries

1.1 Characterization of tension structure

Tension structures are those in which the main load-carrying members transmit loads to the foundation or support system by tensile stresses with no compression or flexure allowed. Their cross-sectional dimensions and method of fabrication are such that their out-of-plane shear and flexural rigidities, as well as their buckling resistance, are negligible. They are load-adaptive in that members change geometry to accommodate changes in load rather than increase stress levels. Tension structures can be comprised of membranes, cables or both. They include air-supported structures, pneumatic shells, prestressed membranes, cable networks, suspension cables, guyed towers and temporary shelters, among others. There are two wide classes of tension structures: cable structures, comprising uniaxially stressed members, and membrane structures, comprising biaxially stressed members. According to [32], these two general categories can be split into many more. Nevertheless, in this research we will focus on:

- Cable networks, in which prestressed segments are connected in a curved surface and loaded predominantly normal to that surface, i.e., suspended nets.
- Prestressed membranes in which fabric or rubber-like sheets are stretched over rigid members and/or perimeter cables, i.e., tents,canopy.

Because of the inherent nonlinear nature of tension structures, conventional linear analysis, which assumes small elastic deformations and displacements, is not applicable. Over the last few decades, considerable mathematical and computational development of suitable analysis techniques has been undertaken. Among the enormous amount of advantages -see [32] and [31]- that the use of this kind of structures entail, it is important to point out the following ones:

1. They are lightweight and easy to erect, transport and dismantle.

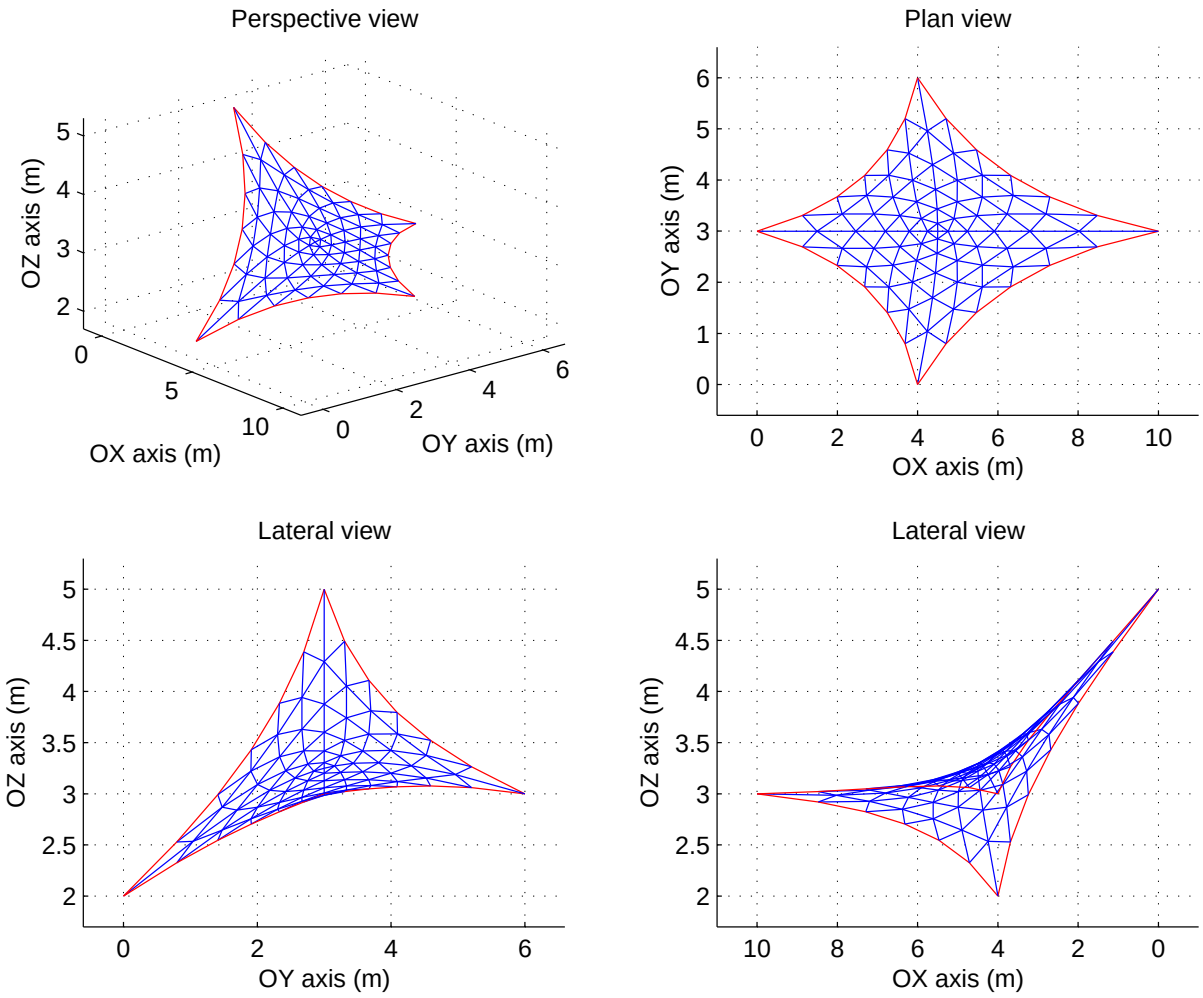

Figure 1.1: Cable Reinforced Membrane Structure 1

2. They can be fabricated in a factory, which provides low installation costs.

3. The environmental loads are efficiently undergone by tensile stresses without the appearance of neither bending nor twisting.

4. They are load-adaptive, in such a way that they will modify its geometry to adapt properly to the applicable loads.

5. They contribute environmentally to a better and sustainable development.

These tension structures are achieving an increasing acceptance level in our society, for example, because of their aesthetic qualities and speed of erection. A large number of tensioned membranes are reinforced by means of interior and perimeter cables. At the same time, compressive rigid members such as masts, are assembled with the global structure in order to provide the adequate stability. The design of cable reinforced prestressed membranes follows a three-stage procedure, involving:

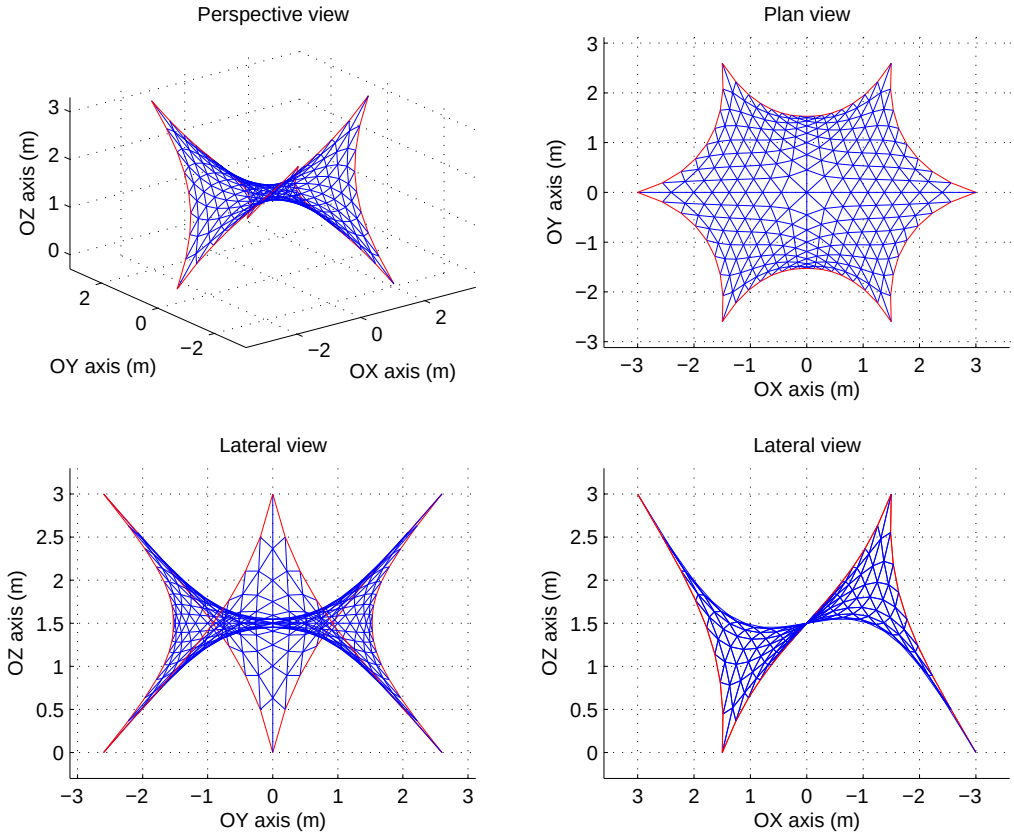

Figure 1.2: Cable Reinforced Membrane Structure 2

1. Form-finding
2. Patterning
3. Static Analysis

In this thesis, we will deal with the first and third of the above issues, specially focusing on the latter. The static analysis is a continuation of the form finding process, in which stresses and strains are calculated under imposed external loads. The problem is geometrically non-linear. The procedure begins with the form-found shape of the structure, which is initially in equilibrium. Static loads are sub-sequentially applied, and a new state of equilibrium is encountered. The procedure has to follow an incremental-iterative scheme, in which displacements and stresses are calculated from the acting loads. Among the wide variety of loads that can be applied on a cable reinforced pre-stressed membrane, two main categories can be underlined:

- Prestressed loading, which is applied with the purpose of serving the role of maintaining an equilibrium geometry for further calculations.

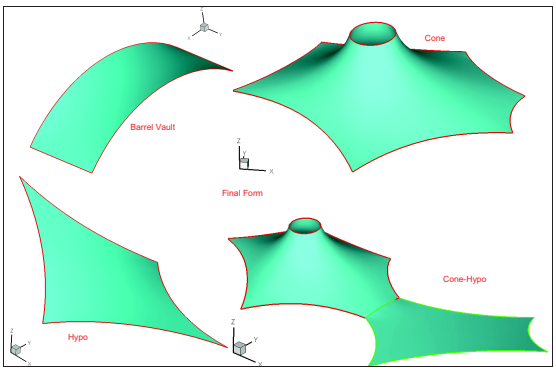

Figure 1.3: Basic geometry shapes used in Tension structures

- In-service loading, where a diverse group of loads can be framed, namely, snow loading, wind loading, live loading, dead loading and so on.

1.2 State of the Art

In tension structures, cable networks and prestressed membranes, form part of a newly and increasing structural technology, which is enabling architects and civil engineers to develop new structural models. These designs are often characterized by their elegance and austerity. These structures, whose main trait is its small thickness, can adopt varied spatial geometries.

The description of the different geometry of space curve and the of surfaces is an important aspect of the mechanics of the tension structures. Because of the dead weight, cable segment are continuously curved in the absence of the other distributed loads e.g weight, to the maintain their shapes.

For membrane structures, the surface curvature is described by the so called gaussian curvature G -see [7], which is the inverse product of the two principal radii of the curvature of the surface. If $G > 0$, the surface is called synclastic, elliptic, or positive gaussian, and the centre of curvature in the two principal directions lie on the same side of the surface. For e.g., spheres require external load e.g pressure or dead weight, to maintain the prestress configuration. If the $G < 0$, the surface is called anticlastic, hyperboilic, saddelike, or negative gaussian and the centre of the curvature lie on the opposite side of the surface. For e.g. hyperboloids do not require external loads: the opposing curvature provides counterstressing such as for sagging-hogging cable combination. If $G = 0$, the surface is called developable, parabolic, or zero-gaussian and at least one radius of curvature is infinite e.g. cylinder

Various materials can be used in the fabrication of a tension structure, such as hyper-elastic (rubber like) materials, fabrics, composites etc.

Hyper elastic materials are highly nonlinear in nature and can sustain large strains. Because of the low stiffness and strength properties they are have limited application.

Fabrics for tension membranes are usually constructed from natural fibers such as cotton (canvas fabric), ceramics (glass fiber) and synthetic organic fibers such as polyester. In order to improve waterproofing and durability, a range of plastic coatings has been developed:

- PVC (polyvinyl chloride) coated polyester.
- PTFE (polytetrafluorethylene) coated glass fiber
- Silicone-coated glass.

The term membrane is quite generic and used to describe compositions of extremely thin sheets to form into flat or curved surfaces. They transmit loads to the supporting medium by means of planar direct and shear stresses. Their bending and transverse shear rigidities are negligible. Even though reinforced and prestressed concrete membranes, subjected to compression stresses, can be included into this category, their study exceeds the scope of this thesis.

As a first approximation, the moderate displacements-small strain linear elasticity theory was used by author such as [29]. The equilibrium equations are established on the final, yet unknown, displaced configuration which does not coincide with the initial unstressed configuration. This ends up in the inclusion of a geometrical nonlinearity within the problem.

Finally, and as a second approach, the theory of hyperelastic membranes, as for example, [32] treats the problem from an exact analytical viewpoint, arriving after complex algebraic manipulations to final formulae of difficult application. Some simplicity, although not much, may be accomplished if the Von Karman compatibility equations are used -see [29]. Regardless of the important implications of this approach into the theoretical understanding of these structures, a main disadvantage is that it results in a nonlinear partial differential equations of impossible analytical solution. Because of this lack of numerical results, variational approaches ought to be taken into consideration as the best route to provide feasible solutions from a practical standpoint. The Galerkin approach, semidiscretized by means of the Finite Element Method (FEM), seemingly provides the best results.

The structural analysis of tension membranes is usually divided into two different stages, according to the loads acting on the membrane, namely, prestressed loading or live loading. The first of the former stages, commonly known as form finding problem, addresses the question of the surface geometry of a fabric tensioned between given boundaries. According to [19], different computational methods can be regarded in this category:

1. "Force density method", where [20] reviews the method proposed by himself in 1971.
2. "Grid method", which is a slight modification of the above method, initiated by Siev and Eidelman in 1964 and formally presented by [19].
3. "Smoothing method"

The first two of the above methods result in a spatial discretized system of algebraic linear equations, whereas the latter corresponds to a final nonlinear system of equations. All of the mentioned techniques were developed for cable networks.

This shape finding problem has been usually related to the search for optimum or minimal surfaces, whose basics are detailed in [7].

Once an initial equilibrium shape is obtained, the analysis of the membrane under external loads must be carried out. Traditionally, cables were adopted as the initial structural, starting from which the overall prestressed membrane could be deployed. The analytical study of cables themselves is reviewed in [16], [32] and [6].

The Finite Element Method or a simple matrix analysis cables networks were the numerical schemes followed to achieve numerical outcomes. see [32], [6], [30] and [19].

The need for efficient membrane elements are essential for solving large-scale industrial problems such as the analysis of structures in civil, mechanical, naval and airspace engineering. Rotation free elements provide one of the means to achieve efficient computation for large scale problem. The basic idea of this formulation is to use the deflection as the only nodal variable for bending analysis. Most of the works on Rotation free elements were developed for plates and shell see. [27], [22], [14], [26] and [9]. More recently multi-purpose general rotation free element based on the thin Kirchhoff-love type shells were presented. where the calculation of the curvature to determine bending strains were based on the discrete nodal directors. see [17].

1.3 Scope of the thesis

The main aim of this thesis is the development of rotation free element for membrane analysis. The present works follows the work of [11], Where the existing formulation for cable and membrane element is used and a new formulation for the rotation free element is developed. In order to test the robustness and reliability of the final formulation some numerical examples was performed.

The general principle and equation will be described in this thesis. There are three stages in the design of the membrane structures, namely form finding, loading analysis and patterning. For detailed account of the finite element procedure for form finding see [20]. The loading analysis is the prolongation of the form finding stage but the stresses and the strains are calculated with imposed loads. The initial equilibrium shape is formed

by displacing the support points to their target heights from the flat membrane mesh. Basically, the applied algorithm is a nonlinear Finite Element Method analysis with an incremental-iterative scheme, in which the stress and the displacement are calculated from the acting loads. It includes continuum equations and the material constitutive equations. In this thesis, as the membrane material is assumed to be hyperelastic, the Saint Venant-kirchhoff model is chosen as the constitutive model to represent the moderate strain behavior of the membrane. The calculation of the bending stiffness is carried out for patch of two elements. The curvature is approximated by Central finite difference. Finally by adding the bending stiffness through rotation free elements the analysis is carried out.

The present coding allows to model for point and uniform loads and two different boundary conditions namely simply supported and clamped condition. The algorithm also contains a series of numerical technique for the iterative solution of the resulting nonlinear equations: the Steepest Descent method, Conjugate Gradient and Newton-Rapson method.

1.4 Layout of the thesis

To achieve the scientific objectives detailed in the previous section, this thesis will be divided into different chapters which are outlined as follows:

- Chapter II reviews Firstly the strong formulation of a structural problem starting from an initial unstressed configuration in total Lagrangian format. The weak form of the structural problem is presented. finally semidiscretization of the weak form is carried out.

- The Chapter III details the formulation of the cable, membrane element and followed by a simple example. With each of the section detailing the Finite element semidiscretization of the previously obtained weak form. Cables is semidiscretised by means of simple two node linear element. The membrane is semidiscretised by means of the Lagrangian mesh (linear triangular element) geometry.

- Chapter IV details the formulation of Rotation Free Membrane Element. Based on the Lagrangian mesh with only three translation degree of freedom at each node, the bending contribution due to external load based on the curvature of each patch is calculated. Finally the total stiffness matrix and internal force vector of the system is obtains by contribution from each of the element (Cable, Membrane and Bending Element). To check the robustness of the formulation simple numerical examples are performed.

- Chapter V Conclusion and Further research.

Chapter 2

General Formulation of the problem

2.1 Introduction

The numerical resolution of any structural problem by means of a computational technique is comprised of four successive stages:

1. Posing the boundary value problem (BVP), which consists of the system of partial differential equations along with the boundary conditions. This stage is named as Strong Formulation.

2. Posing the Principle of Virtual Work or Principle of Virtual Power to obtain the Weak Formulation of the problem.

3. Posing the space-time numerical scheme in order to transform the continuum problem into a discrete problem.

4. Computational implementation, whereby the mathematical formulation of the discretized problem is converted into a computer code by means of an algorithmic language.

This chapter is organized as follows. Sections 2.1.1 and 2.1.2 will summarize the conservation equations or balance laws of a continuum in terms of Lagrangian formulation. No attention will be devoted at this moment, towards the required continuity and boundary conditions, either Dirichlet, Neumann or mixed conditions. The following section will present in brief the strong formulation of the structural problem: prestressed membranes with immediate applications in Civil Engineering. The membranes will be considered to undergo large displacements but moderate strains. Therefore, nonlinear continuum mechanics principles dealing with large deformations on prestressed bodies will be accounted for. The constitutive model adopted for the material will be a prestressed Saint Venant-

Kirchhoff hyperelastic one. see for more details [11], [5] and [15] on basics of nonlinear continuum mechanics.

2.1.1 Lagrangian formulation of the balance laws

For the prospective structural analysis carried out in this research, the formulation of the balance laws in a Lagrangian description results to be even more fundamental. These equations can be depicted as follows:

1. Mass conservation.
$$\rho(\mathbf{X},t) = \rho_0(\mathbf{X}) \qquad \rho J = \rho_0 \tag{2.1}$$

2. Linear momentum conservation
$$\rho_0 \frac{\partial v_i(\mathbf{X},t)}{\partial t} = \frac{\partial P_{ji}}{\partial X_j} + \rho_0 b_i \qquad \rho_0 \dot{\mathbf{v}} = \nabla_0 \cdot \mathbf{P} + \rho_0 \mathbf{b} \tag{2.2}$$

3. Angular momentum conservation
$$F_{ik}P_{kj} = F_{jk}P_{ki}, \quad S_{ij} = S_{ji}; \quad \mathbf{F}\cdot\mathbf{P} = \mathbf{P}^T\cdot\mathbf{F}^T, \quad \mathbf{S} = \mathbf{S}^T \tag{2.3}$$

4. Energy conservation (First law of Thermodynamics)
$$\rho_0 \frac{\partial u_{int}}{\partial t} = \frac{\partial F_{ji}}{\partial t} P_{ij} = \frac{\partial E_{ij}}{\partial t} S_{ij} \qquad \rho_0 \dot{u}_{int} = \dot{\mathbf{F}}^T : \mathbf{P} = \dot{\mathbf{E}} : \mathbf{S} \tag{2.4}$$

where:
ρ_0 represents the continuum's density at the initial configuration.
ρ represents the continuum's density at the final configuration.
$\mathbf{F}$ represents the deformation gradient tensor.
J is the jacobian of the transformation or determinant of the deformation gradient tensor $\mathbf{F}$.
$\mathbf{v}$ represents the velocity field.
∇_0 represents the divergence operator respect to the material coordinates $\mathbf{X}$.
$\mathbf{P}$ represents the nominal stress tensor, which is also known as the transpose of the First-Piola Kirchhoff stress tensor.
$\mathbf{S}$ stands for the second Piola-Kirchhoff stress tensor.
$\mathbf{E}$ represents the Green-Lagrange strain tensor.
$u_{int}$is the functional which represents the internal strain energy accumulated in the continuum per unit of mass.
Some of the key points are:

- The symmetrical feature of the second piola-Kirchhoff stress tensor $\mathbf{S}$. This is not the case of the nominal stress tensor $\mathbf{P}$.

- With respect to the internal power, two different conjugate pairs can be set up, namely, the nominal stress tensor $\mathbf{P}$ with the transpose of the ratio of the deformation gradient tensor $\dot{\mathbf{F}}^T$, and the second Piola-Kirchhoff stress tensor $\mathbf{S}$ with the ratio of the Euler-Lagrange strain tensor $\dot{\mathbf{E}}$.
- Thermal effects were neglected when deriving the energy conservation equation.

2.1.2 Constitutive Model

Apart from the equilibrium and compatibility equations, in order to establish correctly the strong formulation of the problem, constitutive equations must be taken into consideration. This set of equations relates stresses and strains in a specific way according to the selected material's constitutive model. The final constitutive constitutive equations must satisfy certain physical principles. For example, the equations must obviously be objective, that is, frame invariant. For a detailed explanation of this principle, see for details [21], [2] and [15].

In this thesis, the constitutive equations will be established in the context of a hyperelastic material, whereby stresses are derived from a stored elastic energy function (Helmholtz's free energy functional). On account of this fact, the Helmholtz's free energy functional can be expressed as a potential for the stress tensor as follows:

$$\mathbf{S} = \frac{\partial w_{int}(\mathbf{E})}{\partial \mathbf{E}}, \qquad S_{ij} = \frac{\partial w_{int}}{\partial E_{ij}} \tag{2.5}$$

Where:

1. $\mathbf{S}$ stands for the second Piola-Kirchhoff stress tensor.
2. $\mathbf{E}$ represents the Green-Lagrange strain tensor.
3. w_{int} symbolizes the functional which stores the internal strain energy per unit initial volume, where $w_{int} = \rho_0 u_{int}$, according to the equation 2.1

Numerous engineering applications and, in particular, the one which is of concern throughout this research, namely, prestressed membranes, undergo moderate strains in spite of being subjected to large deformations. This means that the major contribution to the deformation gradient tensor comes from its rotating component. The behaviour of these specific materials is completely gathered by means of a mere extension of the small deformations linear-elastic law. As a result of this, the constitutive equations of this sort of hyperelastic materials, known as Saint Venant-Kirchhoff materials, or simply, Kirchhoff materials, turn out to be:

$$S_{ij} = \mathcal{C}_{ijkl} E_{kl} \qquad \mathbf{S} = \mathcal{C} : \mathbf{E} \tag{2.6}$$

As can be noted from comparing equation 2.6 with the classical small deformations linear-elastic constitutive equation, the second Piola-Kirchhoff stress tensor $\mathbf{S}$ and the Green-Lagrange strain tensor $\mathbf{E}$ have been substituted for the Cauchy stress tensor σ and the small strain tensor ϵ,respectively.

Furthermore, the Helmholtz's free energy functional for this particular constitutive model yields:

$$w_{int} = \frac{1}{2} S_{ij} E_{ij} = \frac{1}{2} \mathcal{C}_{ijkl} E_{kl} E_{ij} \qquad w_{int} = \frac{1}{2} \mathbf{S} : \mathbf{E} = \frac{1}{2} \mathbf{E} : \mathcal{C} : \mathbf{E} \tag{2.7}$$

Within the Saint Venant-Kirchhoff hyperelastic materials, this investigation will deal with those associated with an isotropic response. Hence, equation 2.6 can be rewritten in terms of the Lamè constants λ and μ in the following manner:

$$S_{ij} = \lambda E_{kk} \delta_{ij} + 2\mu E_{ij} \qquad \mathbf{S} = \lambda tr(\mathbf{E}) \mathbf{I} + 2\mu \mathbf{E} \tag{2.8}$$

Analogously, the above formula can be expressed as a function of the classical engineering constants, namely, Young modulus E and Poisson ratio ν, which can be related to the aforementioned parameters λ and λ as follows:

$$\lambda = \frac{\nu E}{(1+\nu)(1-2\nu)} \qquad \mu = \frac{E}{2(1+\nu)} \tag{2.9}$$

2.1.3 Total Lagrangian Formulation

The initial prestressed state $\mathfrak{R}_{pret}$ and a final in service loading state $\mathfrak{R}$ due to the consideration of live and dead load. Henceforth, the coordinates of any body's particle, in both prestressed and final loaded states, are related by means of the incremental displacement field $\mathbf{u}$ as follows:

$$\mathbf{x} = \mathbf{X}^{pret} + \mathbf{u}, \qquad x_i = X_i^{pret} + u_i \tag{2.10}$$

According to this nomenclature, the strong formulation of the problem in a Lagrangian description with respect to the prestressed configuration is summarized in figure 2.1. The configurations $\mathfrak{R}_{pret}$ represents a material body of domain V^{pret} with frontier Γ^{pret}. As can be observed, the super index (') has been suppressed for the sake of simplicity.

1. Balance of the linear momentum

$$\frac{\partial P_{ji}}{X_j^{pret}} + \rho^{pret} b_i = 0 \quad in \quad V^{pret} \tag{2.11}$$

2. Transformation of stress tensor

$$J\sigma_{ij} = \frac{\partial x_i}{\partial X_k^{pret}} P_{kj} = \frac{\partial x_i}{\partial X_k^{pret}} \frac{\partial x_j}{\partial X_l^{pret}} S_{kl}; \qquad J = det(\frac{\partial x_i}{\partial X_j^{pret}}) \tag{2.12}$$

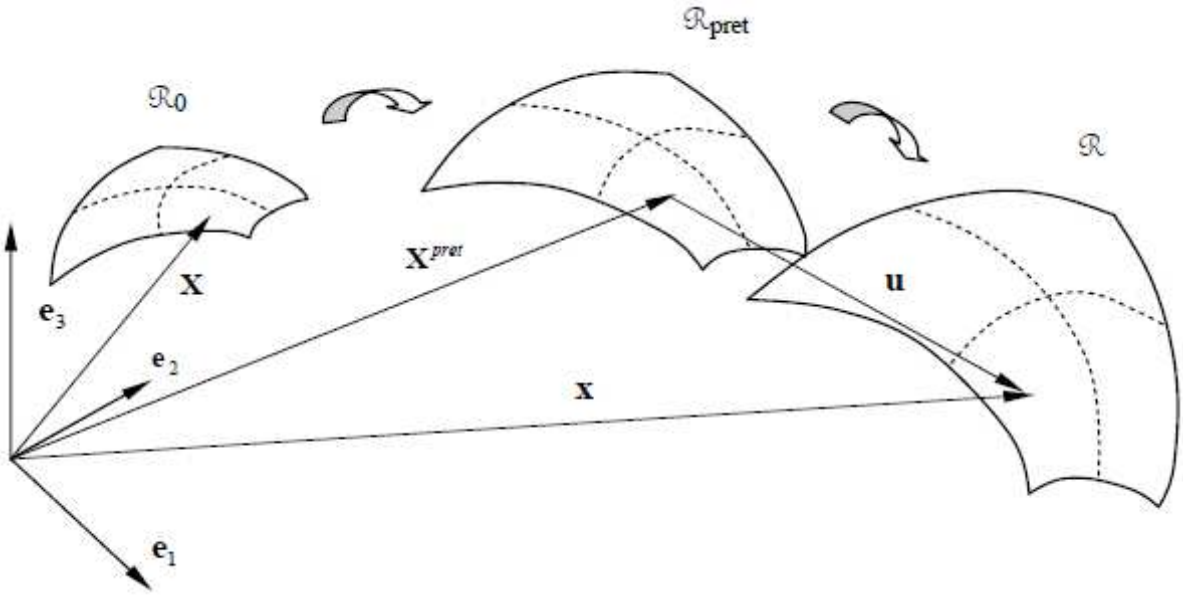

Figure 2.1: Motion of a prestress body

3. Green-Lagrange strain tensor

$$E_{ij} = \frac{1}{2}(\frac{\partial x_k}{\partial X_i^{pret}}\frac{\partial x_k}{\partial X_j^{pret}} - \delta_{ij}) \tag{2.13}$$

4. Constitutive law

$$S_{ij} = \sigma_{ij}^{pret} + \mathcal{C}_{ijkl}E_{kl} \tag{2.14}$$

5. internal strain energy functional per unit volume of the prestress configuration.

$$w_{int} = \sigma_{ij}^{pret}E_{ij} + \frac{1}{2}\mathcal{C}_{ijkl}E_{ij}E_{kl} \tag{2.15}$$

6. Boundary Condition

$$t_i = P_{ji}n_j^{pret} = \bar{t}_i \quad on \quad \Gamma_{t_i}^{pret} \qquad u_i = \bar{u}_i \quad on \quad \Gamma_{u_i}^{pret} \tag{2.16}$$

To obtain the Total Lagrangian Formulation of the problem, the balance of linear momentum equation is multiplied by a test function δu and then integrated over the volume of the prestressed configuration:

$$\int_{V^{pret}} \delta u_i(\frac{\partial P_{ji}}{\partial X_j^{pret}} + \rho^{pret}b_i)dV = 0 \tag{2.17}$$

The integral equation represents a weighted residual method. As can be noted,a good approximation to the exact solution would imply that the conservation of linear momentum is nearly satisfied at all points of the domain V^{pret}. Amid the different weighted residual methods, the Galerkin approach will be the selected one, whose complete development

may be encountered in: [24], [18] and [2]. By applying, thus, the Gauss or divergence theorem along with the well known chain rule, the weak form may be developed in a Total Lagrangian Format (TLF). Neglecting inertia forces, this gives:

$$\delta W_{int}(\delta u_i, u_i) = \delta W_{ext}(\delta u_i, u_i) \tag{2.18}$$

$$\delta W_{int} = \int_{V^{pret}} \delta F_{ij} P_{ji} \quad dV = \int_{V^{pret}} \delta \mathbf{F}^T : \mathbf{P} dV \tag{2.19}$$

$$\delta W_{ext} = \int_{V^{pret}} \delta u_i \rho^{pret} b_i \quad dV + \int_{\Gamma^{pret}} \delta u_i \bar{t}_i \quad d\Gamma$$

$$= \int_{V^{pret}} \delta \mathbf{u}^T \cdot \rho^{pret} \mathbf{b} \quad dV + \int_{\Gamma^{pret}} \delta \mathbf{u}^T \cdot \bar{\mathbf{t}} \quad d\Gamma \tag{2.20}$$

Equation 2.19 may be rewritten as a function of the second Piola-Kirchhoff stress tensor as well as the Euler-Lagrange strain tensor, as it can be noted from the following derivation:

$$\delta \mathbf{F}^T : \mathbf{P} = \delta F_{ij} P_{ji} = \delta F_{ij} F_{ik} S_{jk} = \frac{1}{2}(\delta F_{ij} F_{ik} + \delta F_{ik} F_{ij}) S_{jk} = \delta E_{jk} S_{jk} = \delta \mathbf{E} : \mathbf{S} \tag{2.21}$$

where in order to obtain the above formula, we have made use of the fact that the inner product of a symmetric and a skew-symmetric tensor is null. As can be detected, the work conjugacy property of the tensors $\mathbf{S}$ and $\mathbf{P}$ with $\mathbf{E}$ and $\mathbf{F}^T$, respectively, has been deduced.

From a structural standpoint, equation 2.18 is known as **Principle of Virtual Work** and physically it represents a set of equilibrium equations in a global level for the whole domain V^{pret}, unlike the strong form 2.11 where the equilibrium is guaranteed in a local level.

From equations 2.18 to 2.21, we can observe that the Total Lagrangian Formulation requires to know the referential or material coordinates of the continuum configuration $\mathfrak{R}_{pret}$ and to refer all the scalar, vector and tensor magnitudes with respect to it. Finally, the numerical integration will be carried out over the volume V^{pret} and its contour Γ^{pret}.

2.2 Finite element semidiscretization

The weak form equation obtained formerly may be combined with the finite element of the displacement field in terms of the nodal values and the shape function N^I as

$$u_i = u_i^I N^I, \qquad i = 1, 2, 3 I = 1 \cdots N \text{ nodes} \tag{2.22}$$

This enables the nodal equivalent internal and external force vectors, $\mathbf{f_{int}}$ and $\mathbf{f_{ext}}$, respectively, to be obtained in the a straightforward manner for a given node I in the tensor notation as;

$$f_{int}^I = \int_{\Omega^{pret}} P_{ij} \frac{\partial N^I}{\partial X_j^{pret}} dV = \int_{\Omega^{pret}} F_{ik} S_{kj} \frac{\partial N^I}{\partial X_j^{pret}} dV \tag{2.23}$$

$$f_{ext}^{I} = \int_{\Omega^{pret}} b_i N^I dV + \int_{\Omega^{pret}} \bar{t}_i N^I d\Gamma \tag{2.24}$$

Or in the matrix notation it can be represented as,

$$f_{int}^{I} = \int_{\Omega^{pret}} \mathbf{P}^T \nabla N^I dV = \int_{\Omega^{pret}} FS\nabla N^I dV \tag{2.25}$$

$$f_{ext}^{I} = \int_{\Omega^{pret}} \mathbf{P} N^I dV + \int_{\Omega^{pret}} \bar{\mathbf{t}} N^I \Gamma \tag{2.26}$$

Assembling these forces for all the nodes of the lagrangian mesh gives the global equilibrium equations

$$f_{int}^{I} = f_{ext}^{I} \Rightarrow = f_{res}^{I} = f_{int}^{I} - f_{ext}^{I} = 0 \tag{2.27}$$

Where f_{int} is the global vector of the internal force, f_{ext} is the global vector of the external force, f_{res} is the global vector of the residual force. This last vector represent clearly the out of balance force as a result of the strong nonlinearlity contained into the structural problem.

The set of the equation depicted at 2.27 presents a geometrically nonlinear feature, so an iterative solution scheme will be required. Among all the available available methods, the second-order Newton-Rapson one accomplishes the best convergence properties. The total tangent stiffness matrix required by the later one is formed by the linearizing the global equilibrium equation 2.27 in the direction of the incremental displacement $\mathbf{u}$.

By carrying out the linearization of the global vector of the internal force, it turns out to be,

$$d\mathbf{f}_{int}^{I} = d\mathbf{f}^{mat^I}{}_{int} + d\mathbf{f}^{geo^I}{}_{int} = (\mathbf{K}^{mat^{IJ}} + \mathbf{K}^{geo^{IJ}}) d\mathbf{u}^J \tag{2.28}$$

Where $(\mathbf{K}^{mat^{IJ}})$ and $(\mathbf{K}^{geo^{IJ}})$ stands for the elemental material or constitutive stiffness matrix and the elemental geometrical or initial stress stiffness matrix, respectively. Each one of the these matrices can be expanded and represented in tensor notation as follows.

$$K^{mat^{IJ}}{}_{ij} = \int_{V^{pret}} F_{ik} \frac{\partial N^I}{\partial X_p^{pret}} \mathcal{C}_{pklm} F_{jl} \frac{\partial N^J}{\partial X_m^{pret}} dV \tag{2.29}$$

$$K^{geo^{IJ}}{}_{ij} = \delta_{ij} \int_{V^{pret}} \frac{\partial N^I}{\partial X_l^{pret}} S_{lk} \frac{\partial N^J}{\partial X_k^{pret}} dV \tag{2.30}$$

Formulas 2.29 and 2.30 represent two different components of the equivalent internal nodal forces vector differential $d\mathbf{f}_{int}^{I}$,which may be described as:

1. Equation 2.29 stands for the variation of the second Piol-Kirchhoff stress tensor with respect to the displacements field of the mesh, resulting in the well known symmetric **material stiffness matrix** .

2. Equation 2.30 accounts for the fact that the equilibrium was set up on the deformed configuration and not on the initial one, resulting in the **geometric stiffness matrix** or **initial stress matrix** , which is a diagonal matrix.

Those matrices are added to yield the **total tangent stiffness matrix** , that is:

$$\mathbf{K}^{tan^{IJ}} = \mathbf{K}^{mat^{IJ}} + \mathbf{K}^{geo^{IJ}} \tag{2.31}$$

Chapter 3

Element formulation

3.1 Introduction

Among the wide variety of tension structures in Architecture and Civil Engineering, both prestressed membranes and cable networks constitute a very remarkable group. These structures are achieving an increasing acceptance level in our society, for example, because of their aesthetic qualities and speed of erection. A large number of tensioned membranes are reinforced by means of interior and perimeter cables. Thus, the analysis of cable elements can be considered as a previous step for a further and comprehensive study of prestressed membranes. Some References in which the authors has pursued analytical solutions are [25], [32] and [16] and those authors who pursued numerical solution are [32], [30] and [6].

Analogously, throughout the last decades, the state of the art of prestressed membranes shows a broad variety of publications, which might be allocated in three different categories:

1. Basic examples which are analyzed by means of analytical approaches; the strong formulation is solved in domains of simple geometry: see [29], [25], [6] and [32]

2. Membranes which are assimilated to cable networks, whereby orthotropic hyperelastic membranes can be analyzed in a fairly accurate manner. Any of the References mentioned in previous paragraphs are valid examples.

3. The exact continuum approach for large strain non-prestressed membranes is studied in multiple References: [8], [4] and [3]. Recent developments are due to [4] and [13].

The aim of this chapter is to summarize the Total Lagrangian Formulation for cable and membrane element followed by a simple numerical example.

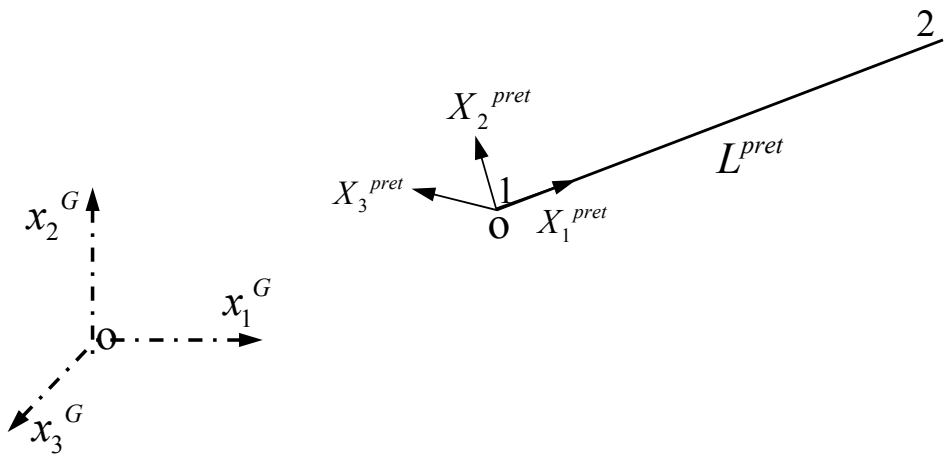

Figure 3.1: Cable Element Description

3.2 Cable Element

The deformation of a cable structure can be described in a standard Lagrangian format by means of a mapping ϕ established between initial configuration $\mathbf{X}$ and the current configuration $\mathbf{x}$ at the time t as $\mathbf{x} = \phi(\mathbf{X}, t)$.

Let us establish, according to figure 3.1, a fixed local coordinate $OX_1^{pret}OX_2^{pret}OX_3^{pret}$ apart from the global co-ordinate system is established for each element. The direction OX_1^{pret} is adapted to move along the longitudinal axis of the cable. According to this criteria, the linear one dimensional shape functions results to be:

$$N^1(X_1^{pret}) = 1 - \frac{X_1^{pret}}{L_1^{pret}} \quad N^2(X_1^{pret}) = \frac{X_1^{pret}}{L_1^{pret}} \tag{3.1}$$

Where L_1^{pret} stands for the initial prestressed length of the cable element. The displacement field and the final spatial coordinates may thus be interpolated in a standard manner as follows

$$u_i = N^1 u_i^1 + N^2 u_i^2 \qquad x_i = N^1 x_i^1 + N^2 x_i^2 \qquad i = 1, 2, 3 \tag{3.2}$$

For simplicity the "pret" superscript will be omitted.
The covariant vectors $\vec{G}_\xi$ is defined as,

$$\vec{G}_\xi = \frac{\partial \mathbf{X}}{\partial \xi} = X^a \frac{\partial N^a}{\partial \xi} = \vec{X}^{12} = X^2 - X^1 \tag{3.3}$$

Covariant and the contravariant vectors has to satisfy the condition,

$$\vec{G}_\xi \cdot \vec{G}^\xi = 1 \Rightarrow \vec{G}^\xi = \frac{\vec{X}^{12}}{\| \vec{X}^{12} \|^2} \tag{3.4}$$

The deformation gradient tensor F can be defined by, for details see [5]

$$F = x^a \otimes \nabla_0 N^a = x^a \otimes \left\{ \left(\frac{\partial \mathbf{X}}{\partial \xi} \right)^{-T} \nabla_\xi N^a \right\} \tag{3.5}$$

Expanding for each node a,

$$= x^1 \otimes \underbrace{\nabla_0 N^1}_{-\vec{G}^\xi} + x^2 \otimes \underbrace{\nabla_0 N^2}_{\vec{G}^\xi} \tag{3.6}$$

$$= \left(x^2 - x^1 \right) \otimes \vec{G}^\xi = \vec{x}^{12} \otimes \vec{G}^\xi \tag{3.7}$$

But deformation gradient tensor F has to be completed in two directions perpendicular to $\vec{G}^\xi$
Thus,

$$F = \vec{x^{12}} \otimes \frac{\vec{X}^{12}}{\| \vec{X}^{12} \|^2} + \vec{\mathbf{n}} \otimes \vec{\mathbf{N}} + \vec{\mathbf{m}} \otimes \vec{\mathbf{M}} \tag{3.8}$$

(where vector $\vec{\mathbf{N}}$, $\vec{\mathbf{M}}$ are the unit vectors $\perp \vec{X}^{12}$)
The Green-Lagrange strain tensor E can be defined as,

$$E = \frac{1}{2} \left(F^T F - I \right) = \frac{1}{2} \frac{\| \vec{x}^{12} \|^2 - \| \vec{X}^{12} \|^2}{\| \vec{X}^{12} \|^2} \left(\frac{\vec{X^{12}}}{\| \vec{X}^{12} \|^2} \otimes \frac{\vec{X^{12}}}{\| \vec{X}^{12} \|^2} \right) \tag{3.9}$$

where the Green-Lagrange strain component E_{11} is,

$$E_{11} = \frac{1}{2} \frac{\| \vec{x}^{12} \|^2 - \| \vec{X}^{12} \|^2}{\| \vec{X}^{12} \|^2} \qquad \text{and} \qquad \vec{\mathbf{N}^{12}} = \frac{\vec{X}^{12}}{\| \vec{X}^{12} \|^2}$$

The Second-Piola Kirchhoff stress tensor S can be represented as,

$$S = E\, E_{11}\, \vec{\mathbf{N}}^{12} \otimes \vec{\mathbf{N}}^{12} \qquad \text{Where } E \text{ is Young's modulus} \tag{3.10}$$

The Equivalent internal nodal force can be expressed,

$$T^a{}_{(e)} = \int_{L_{(e)}} F\, S\, \vec{\nabla}_0 N^a \, d\,\Omega = A\, L_{(e)}\, F\, S\, \vec{\nabla}_0 N^a \tag{3.11}$$

Where L_e is the original elemental length and A is the cross sectional area of the cable element,But

$$S\, \vec{\nabla}_0 N^2 = E\, E_{11}\, \vec{\mathbf{N}}^{12} \otimes \vec{\mathbf{N}}^{12} \vec{G}^\xi = \frac{E\, E_{11}}{\| \vec{X}^{12} \|^2}\, \vec{G}_\xi \otimes \vec{G}_\xi\, \vec{G}^\xi = \frac{E\, E_{11}}{\| \vec{X}^{12} \|^2}\, \vec{G}_\xi \tag{3.12}$$

And

$$F\, S\, \vec{\nabla}_0 N^2 = \left(\frac{\vec{x}^{12}}{\| \vec{X}^{12} \|^2} \otimes \vec{X^{12}} \right) \frac{E\, E_{11}}{\| \vec{X}^{12} \|^2}\, \vec{G}_\xi = \frac{E\, E_{11}}{\| \vec{X}^{12} \|^2}\, \vec{x}_{12} \tag{3.13}$$

$$F\,S\,\vec{\nabla_0 N}^2 = \frac{E\,E_{11}}{\parallel \vec{X}^{12} \parallel^2}\,\vec{x}_{12} \tag{3.14}$$

Substituting Eq. 3.14 into Eq. 3.11, the equivalent internal nodal force at node 1 is,

$$\vec{\mathbf{T}}^1 = \frac{-E\,A}{\parallel \vec{X}^{12} \parallel}\,E_{11}\,\vec{x}_{12} \tag{3.15}$$

Similarly, the equivalent internal nodal force at node 2 is,

$$\vec{\mathbf{T}}^2 = \frac{E\,A}{\parallel \vec{X}^{12} \parallel}\,E_{11}\,\vec{x}_{12} \tag{3.16}$$

Now linearization of equivalent internal nodal forces Equation gives Total Tangent Stiffness Matrix.

$$\frac{\partial \vec{\mathbf{T}}^1}{\partial \vec{x}^{12}} = \mathbf{K}^{12} = \frac{-E\,A}{\parallel \vec{X}^{12} \parallel}\,E_{11}\,\underbrace{\frac{\partial \vec{x^2}}{\partial \vec{x}^{12}}}_{\mathbf{I}} - \frac{-E\,A}{\parallel \vec{X}^{12} \parallel}\,\vec{x^{12}} \otimes \frac{\partial E_{11}}{\partial \vec{x}^2} \tag{3.17}$$

But

$$\frac{\partial E_{11}}{\partial \vec{x}^{12}} = \frac{1}{2\ \parallel \vec{X}^{12} \parallel^2}\frac{\partial\left(\parallel \vec{x}^{12} \parallel^2\right)}{\partial \vec{x}^{12}} = \frac{1}{2\ \parallel \vec{X}^{12} \parallel^2} 2\ \parallel \vec{x}^{12} \parallel\ \vec{\mathbf{n}}^{12} = \frac{\vec{x}^{12}}{\parallel \vec{X}^{12} \parallel^2}$$

So, the total stiffness matrix component $\mathbf{K}^{12}$ is,

$$\mathbf{K}^{12} = \frac{-E\,A\,E_{11}}{\parallel \vec{X}^{12} \parallel}\,\mathbf{I} - \frac{-E\,A}{\parallel \vec{X}^{12} \parallel^3}\,\vec{x}^{12} \otimes \vec{x}^{12} \tag{3.18}$$

Where $\dfrac{-E\,A\,E_{11}}{\parallel \vec{X}^{12} \parallel}\,\mathbf{I}$ is the Geometric Stiffness Component

And

$\dfrac{-E\,A}{\parallel \vec{X}^{12} \parallel^3}\,\vec{x}^{12} \otimes \vec{x}^{12}$ is the Constitutive Stiffness Component

The Geometric Stiffness matrix can also be expressed as,

$$K^{\sigma,a,b}_{(e)} = \int_{L^{(e)}} \left(\vec{\nabla}_0 \mathbf{N}^a\ \cdot S\,\vec{\nabla}_0 \mathbf{N}^b\right) \mathbf{I} d\Omega \tag{3.19}$$

$$\nabla_0 \vec{N}^1\ \cdot\ S\,\nabla_0 \vec{N}^2 = \left(-\vec{G}^\xi\right) \cdot \frac{-E\,E_{11}}{\parallel \vec{X}^{12} \parallel^2}\,\vec{G}_\xi = \frac{-E\,E_{11}}{\parallel \vec{X}^{12} \parallel^2} \tag{3.20}$$

The Geometric Stiffness components can be expressed as,

$$\mathbf{K}^{\sigma\,,\,a\,b} = \frac{-E\,A}{\parallel \vec{X}^{12} \parallel}\,E_{11}\,\mathbf{I} \qquad \mathbf{K}^{\sigma\,,\,a\,a} = \frac{E\,A}{\parallel \vec{X}^{12} \parallel}\,E_{11}\,\mathbf{I} \tag{3.21}$$

$\left(\text{where}\quad \mathbf{K}^{\sigma\,,\,a\,a} \text{ and } \mathbf{K}^{\sigma\,,\,a\,b} \quad \text{are Initial Stress Stiffness components}\right)$

Finally, for a cable element the total stiffness matrix components are given by,

$$\mathbf{K}^{a,b} = (-1)^{a,b}\left\{\frac{E\,A\,E_{11}}{\parallel \vec{X}^{12} \parallel}\,\mathbf{I} + \frac{E\,A}{\parallel \vec{X}^{12} \parallel^3}\,\vec{x}^{12} \otimes \vec{x}^{12}\right\} \tag{3.22}$$

The equivalent nodal internal force is given by,

$$\vec{\mathbf{T}}^a = (-1)^a \ \frac{E\,A}{\parallel \vec{X}^{12} \parallel} \ E_{11}\ \vec{x}_{12} \tag{3.23}$$

Where

$$E_{11} = \frac{1}{2}\left(\frac{\parallel \vec{x}^{12} \parallel^2 - \parallel \vec{X}^{12} \parallel^2}{\parallel \vec{X}^{12} \parallel^2}\right)$$

3.3 Membrane Element Formulation

The membrane is discretized by a number of three noded isoparametric triangular elements with linear shape functions. The geometry of each element in the initial prestressed state, according to the figure 3.2, it can be defined by a plane of unit uniform thickness t bounded by straight lines which intersect at three points called nodes.

A fixed local coordinate $OX_1^{pret}OX_2^{pret}OX_3^{pret}$ is established for each element apart from the global reference frame. It is assumed that the each element lies on the OX_1^{pret} OX_2^{pret} plane of the its local coordinate system. Thus, the displacement field and the current coordinate can be interpolated in terms of the shape functions as:

$$u_i = N^1 u_i^1 + N^2 u_i^2 + N^3 u_i^3 \qquad x_i = N^1 x_i^1 + N^2 x_i^2 + N^3 x_i^3 \qquad i = 1,2,3 \tag{3.24}$$

$$\begin{gathered} N^1(X_1^{pret}, X_2^{pret}) = \frac{1}{2\Gamma^{pret}}(a^I + b^I X_1^{pret} + c^I X_2^{pret} \\ a^I = X_1^{pret\,J} X_1^{pret\,K} - X_1^{pret\,K} X_1^{pret\,J} \\ b^I = X_2^{pret\,J} - X_2^{pret\,K} \\ c^I = X_2^{pret\,K} - X_2^{pret\,J} \\ \Gamma^{pret} = \frac{1}{2}(c^k b^j - c^J b^K) \quad I,J,K = 1,2,3 \end{gathered} \tag{3.25}$$

Where Γ^{pret} stands for area the initial prestressed triangle. Note that the a^I,a^J,a^K are the Zienkiewicz's coefficients. For simplicity the "pret" superscript will be omitted.

The deformation of a membrane structure can be described in a standard Lagrangian format by means of a mapping ϕ established between initial configuration $\mathbf{X}$ and the current configuration $\mathbf{x}$ at the time t as $\mathbf{x} = \phi(\mathbf{X}, t)$. Thus, the following kinematics entities can be defined:

$$C = F^T F \qquad b = F F^T \qquad E = \frac{1}{2}(C - I) \qquad F = \frac{\partial \mathbf{x}}{\partial \mathbf{X}} \qquad J = detF \tag{3.26}$$

where C is the right Cauchy-Green tensor, b is the left Cauchy-Green tensor, E is the Green-Lagrangian strain tensor, F is the deformation gradient tensor and J is the Jacobian of the transformation. For analysis of membrane structures, the constitutive behaviour is established based on the invariants of the strain components within the local

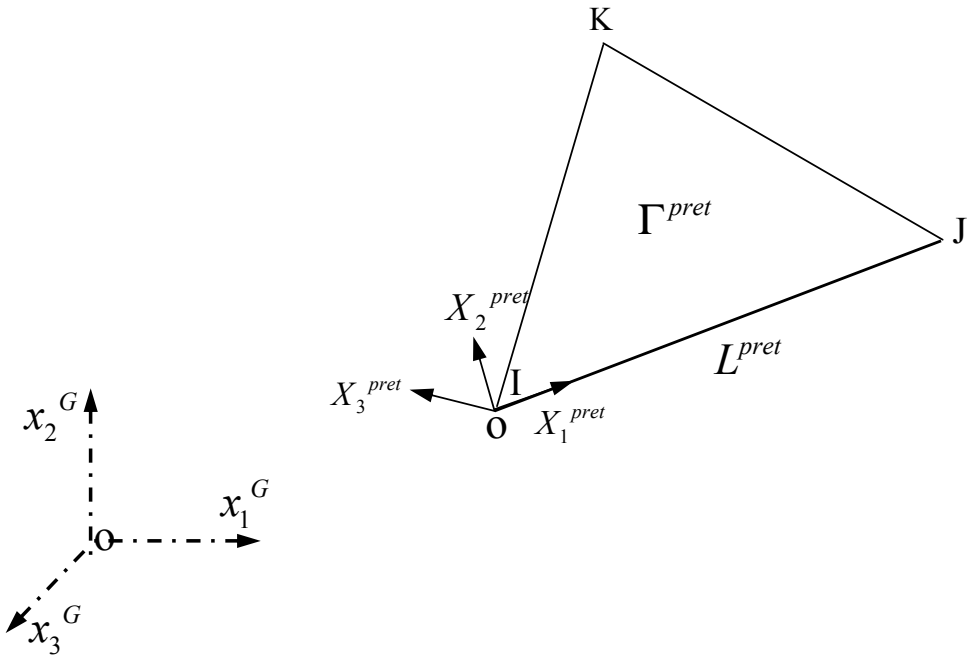

Figure 3.2: Membrane Element Description

tangent plane to the membrane. Therefore, it is standard to define a local Cartesian system of coordinates in such a way that the third direction is aligned with the normal to the local tangent plane of the membrane. In this set of axes, the above tensor C, b, E and F can be formulated as:

$$C = \begin{bmatrix} \bar{C} & 0 \\ 0^T & C_{33} \end{bmatrix} ; b = \begin{bmatrix} \bar{b} & 0 \\ 0^T & b_{33} \end{bmatrix} ; E = \begin{bmatrix} \bar{E} & 0 \\ 0^T & E_{33} \end{bmatrix} ; F = \begin{bmatrix} \bar{F} & 0 \\ 0^T & F_{33} \end{bmatrix} ; \tag{3.27}$$

where $\bar{C}$, $\bar{b}$, $\bar{E}$ and $\bar{F}$ represent the in-plane components of the corresponding deformation tensors. In general, for a three dimensional deformation body, the Saint-Venant Kirchhoff hyperelastic potential ψ is defined in terms of the first two invariants of the Green-Lagrange strain tensor I_E and II_E as follows:

$$\psi(E) = \frac{\lambda}{2} I_E^2 + \mu II_E; \quad I_E = trE; \quad II_E = E : E \tag{3.28}$$

where λ and μ are the well known Lamé coefficients.

The Second Piola-Kirchhoff stress tensor is thus obtained in a standard manner as:

$$S = \frac{\partial \psi}{\partial E} = \lambda I_E I + 2\mu E \tag{3.29}$$

As it has been already mentioned, for tension membrane structure, shear strains transverse to the local tangent plane of the membrane vanish and the strain normal to the local tangent plane can be obtained based on the plane-stress condition. Indeed, as the out-of-plane stress component S must be zero, it yields:

$$S = \begin{bmatrix} \bar{S} & 0 \\ 0^T & S_{33} \end{bmatrix} \; ; \quad S_{33} = (\lambda + 2\mu)E_{33} + \lambda I_{\bar{E}} = 0 \Rightarrow E_{33} = \frac{-\lambda}{\lambda + 2\mu} I_{\bar{E}} \tag{3.30}$$

Where $I_{\bar{E}}$ represent the first invariant of the in-plane Green-Lagrange strain tensor $\bar{E}$. Substituting for E_{33} into formulae 3.29 and 3.28, the in-plane strain energy functional $\bar{\psi}$ and the in-plane second Piola-Kirchhoff stress tensor $\bar{S}$ can be re-expressed in terms of the in-plane Green-Lagrange strain tensor component as:

$$\bar{\psi}(\bar{E}) = \frac{\bar{\lambda}}{2} I_{\bar{E}}^2 + \mu I I_{\bar{E}}; \; \bar{S} = \frac{\partial \bar{\psi}}{\partial E} = \bar{\lambda} I_{\bar{E}} \bar{\mathbf{I}} + 2\mu \bar{E}; \; \bar{\lambda} = \frac{2\lambda\mu}{\lambda + 2\mu} \tag{3.31}$$

Where

$$\mu = \frac{E}{2(1+\nu)} \quad \text{and} \quad \lambda = \frac{E\nu}{(1+\nu)(1-2\nu)}$$

where a new hyper elasticity constant $\bar{\lambda}$ has been introduced. The in-plane Cauchy stress tensor can be obtained in terms of the in-plane components by Piola push forward operation of the tensor $\bar{S}$:

$$\bar{\sigma} = \frac{1}{J} \bar{F} \bar{S} \bar{F}^T = \frac{1}{J} \bar{F} (\bar{\lambda} I_{\bar{E}} \bar{I} + 2\mu \bar{E}) \bar{F}^T \tag{3.32}$$

The in-plane symmetrised constitutive fourth-order tensor can be expressed in indicial form in the initial configuration as:

$$C_{IJKL} = \bar{\lambda} \delta_{IJ} \delta_{KL} + 2\mu \delta_{IK} \delta_{JL} \tag{3.33}$$

The deformation gradient tensor F can be expressed as in [5],

$$F = \frac{\partial \mathbf{x}}{\partial \mathbf{X}} = x^a \otimes \nabla_0 N^a = \mathbf{x}^a \otimes \left\{ \left(\frac{\partial \mathbf{X}}{\partial \xi} \right)^{-T} \nabla_\xi N^a \right\} \tag{3.34}$$

The covariant vectors according figure 3.3 can be expressed as, Where covariant vectors are,

$$\vec{G}_\xi = \frac{\partial \mathbf{X}}{\partial \xi} = X^a \frac{\partial N^a}{\partial \xi} = X^1(-1) + X^2(1) = X^2 - X^1 = \vec{X}^{12} \tag{3.35}$$

$$\vec{G}_\eta = \frac{\partial X}{\partial \eta} = X^a \frac{\partial N^a}{\partial \eta} = X^1(-1) + X^3(1) = X^3 - X^1 = \vec{X}^{13} \tag{3.36}$$

Covariant and the contravariant vectors in ξ direction has to satisfy the condition,

$$\vec{G}^\xi \cdot \vec{G}_\xi = 1 \Rightarrow \frac{\vec{G}_\eta \times \vec{\mathbf{N}}}{\alpha} \cdot \vec{G}_\xi = 1 \tag{3.37}$$

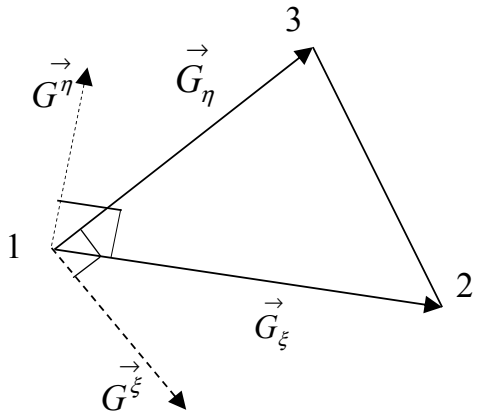

Figure 3.3: Description of Covariant and Contravariant vectors

$$\alpha = \left(\vec{G}_{\eta} \times \vec{\mathbf{N}}\right) \cdot \vec{G}_{\xi} \tag{3.38}$$

$$\vec{G}^{\xi} = \frac{\left(\vec{G}_{\eta} \times \vec{\mathbf{N}}\right)}{\left(\vec{G}_{\eta} \times \vec{\mathbf{N}}\right) \cdot \vec{G}_{\xi}} = \frac{\left(\vec{X}^{13} \times \vec{\mathbf{N}}\right)}{\left(\vec{X}^{13} \times \vec{\mathbf{N}}\right) \cdot \vec{X}^{12}} \tag{3.39}$$

Covariant and the contravariant vectors in η direction has to satisfy the condition,

$$\vec{G}^{\eta} \cdot \vec{G}_{\eta} = 1 \Rightarrow \frac{\vec{\mathbf{N}} \times \vec{G}^{\xi}}{\alpha} \cdot \vec{G}_{\eta} = 1 \tag{3.40}$$

$$\alpha = \left(\vec{\mathbf{N}} \times \vec{G}_{\xi}\right) \cdot \vec{G}_{\eta} \tag{3.41}$$

$$\vec{G}^{\eta} = \frac{\left(\vec{\mathbf{N}} \times \vec{G}_{\xi}\right)}{\left(\vec{\mathbf{N}} \times \vec{G}_{\xi}\right) \cdot \vec{G}_{\eta}} = \frac{\left(\vec{\mathbf{N}} \times \vec{X}^{12}\right)}{\left(\vec{\mathbf{N}} \times \vec{X}^{12}\right) \cdot \vec{X}^{13}} \tag{3.42}$$

Where the normal vectors are defined as,

$$\vec{\mathbf{N}} = \frac{\left(\vec{X^{12}} \times \vec{X}^{13}\right)}{\parallel \vec{X^{12}} \times \vec{X}^{13} \parallel} \quad \text{and} \quad \vec{\mathbf{n}} = \frac{\left(\vec{x^{12}} \times \vec{x}^{13}\right)}{\parallel \vec{x^{12}} \times \vec{x}^{13} \parallel} \tag{3.43}$$

$$\frac{\partial \mathbf{X}}{\partial \xi} = \left\{ \vec{G}_{\xi}\ \vec{G}_{\eta}\ \frac{\vec{G}_{\xi} \times \vec{G}_{\eta}}{\parallel \vec{G}_{\xi} \times \vec{G}_{\eta} \parallel} \right\} \tag{3.44}$$

Where $\frac{\vec{G}_{\xi} \times \vec{G}_{\eta}}{\|\vec{G}_{\xi} \times \vec{G}_{\eta}\|}$ is completed for membrane analysis.

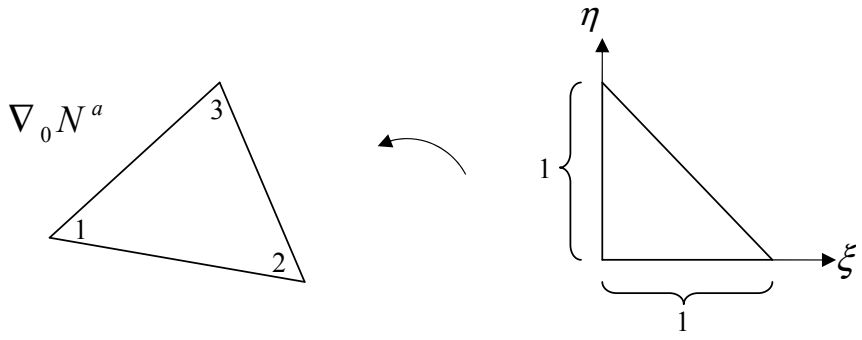

Figure 3.4: Description of Element natural coordinate

Following the figure 3.4, the gradient of the shape function in the element natural coordinate can be expressed as,

$$\nabla_\xi N^a = \begin{Bmatrix} -1 & 1 & 0 \\ -1 & 0 & 1 \\ 0 & 0 & 0 \end{Bmatrix} \tag{3.45}$$

$$\left(\frac{\partial \mathbf{X}}{\partial \xi}\right)^{-T} = \left\{ \vec{G}^\xi \; \vec{G}^\eta \; \frac{\vec{G}^\xi \times \vec{G}^\eta}{\parallel \vec{G}^\xi \times \vec{G}^\eta \parallel} \right\} \tag{3.46}$$

Where $\frac{\vec{G}^\xi \times \vec{G}^\eta}{\|\vec{G}^\xi \times \vec{G}^\eta\|}$ is completed for membrane analysis.

The gradient of the shape function in terms of the contravariant vectors can be expressed as,

$$\nabla_0 N^a = \left\{ \vec{G}^\xi \; \vec{G}^\eta \; \frac{\vec{G}^\xi \times \vec{G}^\eta}{\parallel \vec{G}^\xi \times \vec{G}^\eta \parallel} \right\} \begin{Bmatrix} \frac{\partial N^a}{\partial \xi} \\ \frac{\partial N^a}{\partial \eta} \\ 0 \end{Bmatrix} = \frac{\partial N^a}{\partial \xi} \vec{G}^\xi + \frac{\partial N^a}{\partial \eta} \vec{G}^\eta \tag{3.47}$$

Thus

$$\nabla_0 \mathbf{N} = \left\{ \nabla_0 N^1 \; \nabla_0 N^2 \; \nabla_0 N^3 \right\} = \left\{ -\left(\vec{G}^\xi + \vec{G}^\eta\right) \quad \vec{G}^\xi \quad \vec{G}^\eta \right\} \tag{3.48}$$

The deformation gradient tensor in terms of contravariant vector is represented as,

$$F = \vec{x}^a \otimes \nabla_0 N^a = \vec{x}^1 \otimes \left(-\left(\vec{G}^\xi + \vec{G}^\eta\right)\right) + \vec{x}^2 \otimes \vec{G}^\xi + \vec{x}^3 \otimes \vec{G}^\eta + \vec{n} \otimes \vec{\mathbf{N}} \tag{3.49}$$

The Green-Lagrange strain tensor E is expressed as,

$$E = \frac{1}{2}\left(F^T F - I\right) \tag{3.50}$$

$$S = \frac{\partial \psi}{\partial E} = \bar{\lambda} I_E I + 2\mu E \tag{3.51}$$

Following from the weak formulation from the previous chapters. The Equivalent internal nodal force in the matrix notation can be can be expressed as,

$$T^a{}_{(e)} = \int_{V_0^{(e)}} F\, S\, \vec{\nabla}_0 N^a \, dV \tag{3.52}$$

The Geometric stiffness matrix can be expressed as,

$$\mathbf{K}^{\sigma,a,b}_{(e)} = \int_{V_0^{(e)}} \left(\vec{\nabla}_0 N^a \cdot S\, \vec{\nabla}_0 N^b \right) \mathbf{I} \quad dV \tag{3.53}$$

The Constitutive part of the stiffness matrix can be expressed as,

$$\left[K^{const.,a,b}_{(e)} \right]_{ij} = \int_{V_0^{(e)}} F_{iI} \frac{\partial N^a}{\partial X_J} C^{sym}_{IJKL} \frac{\partial N^b}{\partial X_K} F_{jL} \, dV \tag{3.54}$$

Thus for P1 triangle element the equivalent nodal force are,

$$T^1{}_{(e)} = A\, F\, S\, \vec{\nabla}_0 N^1 = A\, F\, S \left[- \left(\vec{G}^{\xi} + \vec{G}^{\eta} \right) \right] \tag{3.55}$$

$$T^2{}_{(e)} = A\, F\, S\, \vec{\nabla}_0 N^2 = A\, F\, S \left(\vec{G}^{\xi} \right) \tag{3.56}$$

$$T^3{}_{(e)} = A\, F\, S\, \vec{\nabla}_0 \mathbf{N}^3 = A\, F\, S \left(\vec{G}^{\eta} \right) \tag{3.57}$$

Where A is the area of the initial prestressed triangular element.
The Geometric stiffness matrix is given

$$K^{\sigma,2,3}_{(e)} = A \left(\vec{G}^{\xi} \cdot S \vec{G}^{\eta} \right) \mathbf{I} \tag{3.58}$$

$$K^{\sigma,1,2}_{(e)} = A \left\{ \left(- \left(\vec{G}^{\xi} + \vec{G}^{\eta} \right) \right) \cdot S \vec{G}^{\xi} \right\} \mathbf{I} \tag{3.59}$$

The Constitutive stiffness matrix is given by

$$\left[K^{const.,a,b}_{(e)} \right]_{ij} = A\, F_{iI} \frac{\partial N^a}{\partial X_J} C^{sym}_{IJKL} \frac{\partial N^b}{\partial X_K} F_{jL} \tag{3.60}$$

But

$$C^{sym}_{IJKL} = \bar{\lambda} \delta_{IJ}\, \delta_{KL} + 2\, \mu \delta_{IK}\, \delta_{JL} \tag{3.61}$$

Substituting for C^{sym}_{IJKL} into Eq. 3.60 We have,

$$\begin{aligned} \left[K^{const.,a,b}_{(e)} \right]_{ij} &= A\, F_{iI} \frac{\partial N^a}{\partial X_J} \bar{\lambda} \delta_{IJ}\, \delta_{KL} \frac{\partial N^b}{\partial X_K} F_{jL} \\ &\quad + A\, F_{iI} \frac{\partial N^a}{\partial X_J} 2\, \mu\, \delta_{IK}\, \delta_{JL} \frac{\partial N^b}{\partial X_K} F_{jL} \end{aligned} \tag{3.62}$$

$$\left[K^{const.,a,b}_{(e)} \right]_{ij} = A \left\{ \bar{\lambda} F_{iI} \frac{\partial N^a}{\partial X_I} \frac{\partial N^b}{\partial X_L} F_{jL} + 2\, \mu\, F_{iK} \frac{\partial N^a}{\partial X_J} \frac{\partial N^b}{\partial X_K} F_{jJ} \right\} \tag{3.63}$$

But

$$F_{iI}\,\frac{\partial N^a}{\partial X_I} = F\vec{\nabla}_0 N^a \quad \text{and} \quad \frac{\partial N^b}{\partial X_L}\,F_{jL} = F\vec{\nabla}_0 N^b \tag{3.64}$$

And

$$F_{iK}\,\frac{\partial N^a}{\partial X_J} = F\vec{\nabla}_0 N^b \quad \text{and} \quad \frac{\partial N^b}{\partial X_K}\,F_{jJ} = F\vec{\nabla}_0 N^a \tag{3.65}$$

So Finally,

$$\left[K_{(e)}^{const.,a,b}\right]_{ij} = A\left\{\bar{\lambda}F\vec{\nabla}_0 N^a \otimes F\vec{\nabla}_0 N^b + 2\,\mu\,F\vec{\nabla}_0 N^b \otimes F\vec{\nabla}_0 N^a\right\} \tag{3.66}$$

$$C_{IJKL}^{sym} = \frac{1}{4}\left[C_{IJKL} + C_{JIKL} + C_{IJLK} + C_{JILK}\right] \tag{3.67}$$

$$\delta_{IJ}\delta_{KL}^{sym} = \delta_{IJ}\delta_{KL} \tag{3.68}$$

$$\delta_{IK}\delta_{JL}^{sym} = \frac{1}{4}\left\{\delta_{IK}\delta_{JL} + \delta_{JK}\delta_{IL} + \delta_{IL}\delta_{JK} + \delta_{JL}\delta_{IK}\right\} \tag{3.69}$$

Substituting Eq. 3.68 and Eq. 3.69 into Eq. 3.62, expressing second part of the equation term by term we have,

$$\delta_{IK}\delta_{JL} \Rightarrow \left(F\vec{\nabla}_0 N^b\right) \otimes \left(F\vec{\nabla}_0 N^a\right) \tag{3.70}$$

$$\begin{aligned}\delta_{JK}\delta_{IL} \Rightarrow F_{iI}\,\frac{\partial N^a}{\partial X_J}\,\delta_{JK}\,\delta_{IL}\,\frac{\partial N^b}{\partial X_K}\,F_{jL} &= F_{iI}\,\frac{\partial N^a}{\partial X_K}\,\frac{\partial N^b}{\partial X_K}\,F_{jI} \\ &= \left(\vec{\nabla}_0 N^a \cdot \vec{\nabla}_0 N^b\right)\,F\,F^T\end{aligned} \tag{3.71}$$

$$\begin{aligned}\delta_{IL}\delta_{JK} \Rightarrow F_{iI}\,\frac{\partial N^a}{\partial X_J}\,\delta_{IL}\,\delta_{JK}\,\frac{\partial N^b}{\partial X_K}\,F_{jL} &= F_{iL}\,\frac{\partial N^a}{\partial X_J}\,\frac{\partial N^b}{\partial X_J}\,F_{jL} \\ &= \left(\vec{\nabla}_0 N^a \cdot \vec{\nabla}_0 N^b\right)\,F\,F^T\end{aligned} \tag{3.72}$$

$$\begin{aligned}\delta_{JL}\delta_{IK} \Rightarrow F_{iI}\,\frac{\partial N^a}{\partial X_J}\,\delta_{JL}\,\delta_{IK}\,\frac{\partial N^b}{\partial X_K}\,F_{jL} &= F_{LI}\,\frac{\partial N^a}{\partial X_L}\,\frac{\partial N^b}{\partial X_I}\,F_{jL} \\ &= \left(F\,\vec{\nabla}_0 N^b\right) \otimes \left(F\,\vec{\nabla}_0 N^a\right)\end{aligned} \tag{3.73}$$

Thus

$$\begin{aligned}A\,\bar{\lambda}\left(F\vec{\nabla}_0 N^a\right) \otimes \left(F\vec{\nabla}_0 N^b\right) + A\,\frac{2\mu}{2}\left(F\,\vec{\nabla}_0 N^b\right) \otimes \left(F\,\vec{\nabla}_0 N^a\right) \\ + A\,\frac{2\mu}{2}\left(\vec{\nabla}_0 N^a \cdot \vec{\nabla}_0 N^b\right)\,F\,F^T\end{aligned} \tag{3.74}$$

Finally, the Constitutive Stiffness Matrix can be expressed as,

$$\begin{aligned}\left[K_{(e)}^{c,a,b}\right]_{ij} = A\,\bar{\lambda}\left(F\vec{\nabla}_0 N^a\right) \otimes \left(F\vec{\nabla}_0 N^b\right) + A\,\mu\left(F\,\vec{\nabla}_0 N^b\right) \otimes \left(F\,\vec{\nabla}_0 N^a\right) \\ + A\,\mu\left(\vec{\nabla}_0 N^a \cdot \vec{\nabla}_0 N^b\right) FF^T\end{aligned} \tag{3.75}$$

And the Geometric Stiffness Matrix can be expressed as,

$$\left[K^{\sigma,a,b}_{(e)}\right]_{ij} = A\left\{\vec{\nabla}_0 N^a \cdot S\,\vec{\nabla}_0 N^b\right\}\,\mathbf{I} \tag{3.76}$$

The equivalent internal nodal force can be expressed as,

$$T^a{}_{(e)} = A\,F\,S\,\vec{\nabla}_0 N^a \tag{3.77}$$

3.4 Numerical Example

To get better understanding of the membrane elements application for tension structure analysis. Analysis of hyperbolic paraboloid structure will be carried out using the computer program which incorporates the above cable and membrane elements. The structural model comprises of fabric textile and reinforced cables and the analysis will be run for point and snow load conditions according to British standards. The analysis will be developed in three successive stages: namely, form finding problem, prestressing load application and in-service load application.

Form-Finding Stage

In the Form-finding stage, the structure was modeled by adopting three-noded triangular finite elements as shown in the Figures 3.5. The Force Density Method (FDM) has been

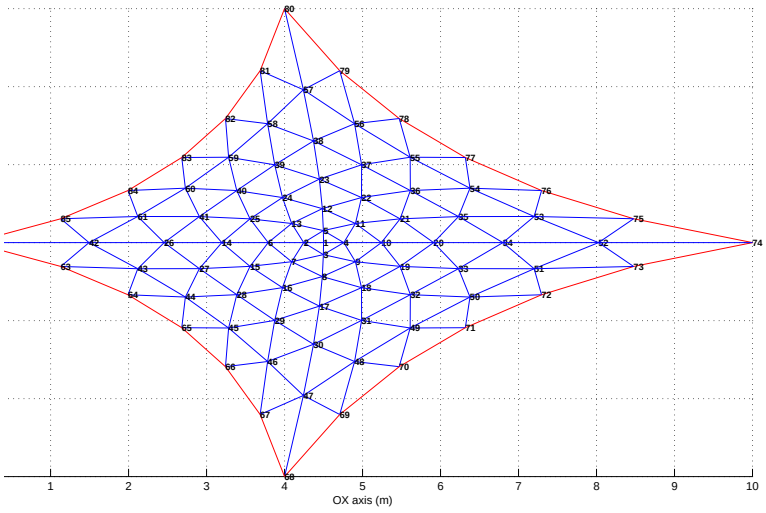

Figure 3.5: Example 1:Initial configuration : Plan view with nodes numbering

employed in order to compute an initial equilibrium shape of the membrane, references [20]. The initial shape of the membrane depends on the location of its corners node,

Boundary Conditions			
Node	X	Y	Z
62	0	3	5
68	4	0	2
74	10	3	3
80	4	6	3

Figure 3.6: Example 1: Boundary condition

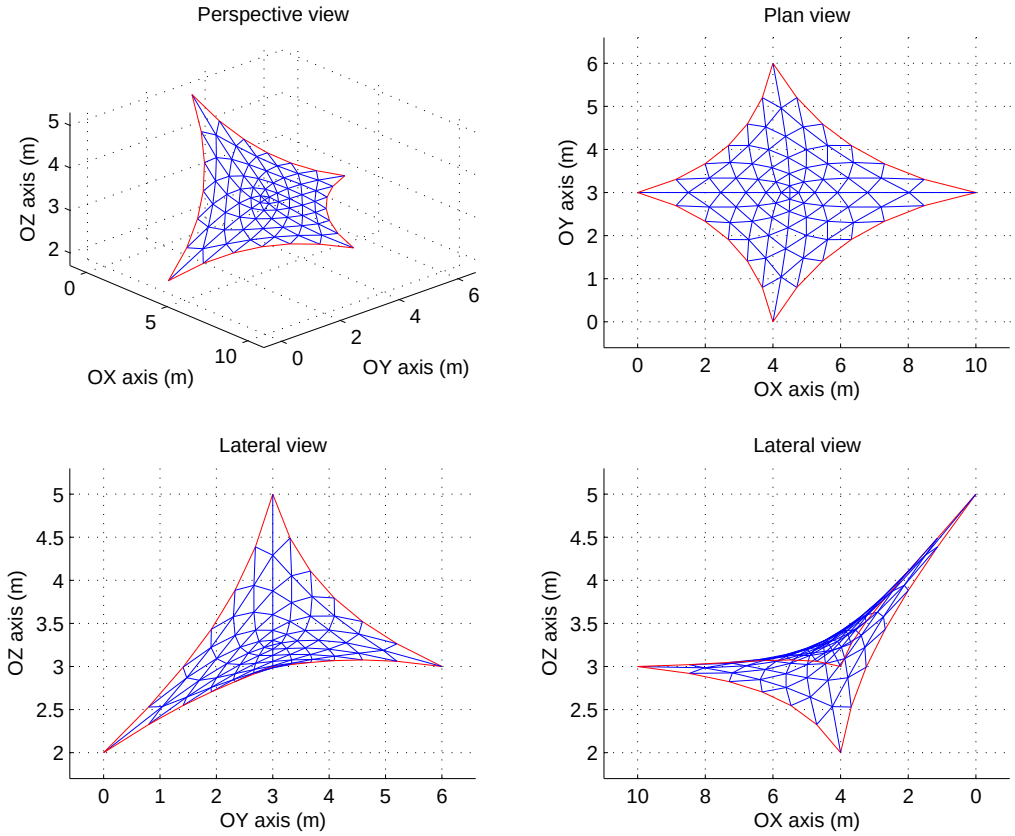

Figure 3.7: Example 1: Four initial configuration views

which are termed as the kinematic boundary conditions. The initial kinematic boundary conditions is as shown in the table 3.6. Figure 3.5 shows the structure has 85 nodes and 144 three-noded finite elements. Figure 3.7 shows the four initial configuration views of the membrane example.

Membrane Material (PVC)

$\rho = 1.76 Mg / m^3$

$Et = 5.0e2 kN / m$

$t = 0.001 m$

$E = 5e5 kN / m^2$

$\upsilon = 0.3$

$\mu = \frac{E}{2(1+\upsilon)} = 1.923077e5 kN / m^2$

$\lambda = \frac{\upsilon E}{(1+\upsilon)(1-2\upsilon)} = 2.884615e5 kN / m^2$

Cable Reinforcement (HSLA Steel)

$\rho = 7.8 Mg / m^3$

$EA = 1.2e4 kN / m$

$A = 7.6531e-5 m^2$

$E = 1.568e8 kN / m^2$

$\upsilon = 0$

$\mu = \frac{E}{2(1+\upsilon)} = 7.84e7 kN / m^2$

$\lambda = \frac{\upsilon E}{(1+\upsilon)(1-2\upsilon)} = 0 kN / m^2$

Figure 3.8: Example 1: Material Property

Boundary Conditions			
Node	u	v	w
62	-0.01	0	0
68	-0.01	0	0
74	-0.01	0.01	0
80	0	0	0

Figure 3.9: Example 1: Prestressing Stage-Boundary Condition

Prestressing Stage And In-Service Load

After the initial shape of the membrane are formed in the form-finding stage, the material properties of the membrane material and cable reinforcement were implemented into the algorithm for modeling purposes. The material properties of the example are shown in Figure 3.8. The prescribed displacements along the corresponding space directions OX, OY and OZ are shown in the Figure 3.9.

In loading stage, pressure load of 2.5 $kN/m2$ have been applied to the prestressed membrane. The snow load data [28] was modeled by applying a uniformly distributed load over the whole surface of the membrane. Figure 3.10, 3.11 and 3.12 shows the displacement along OX, OY and OZ directions and Figures 3.13 and 3.14 shows the Principal Cauchy stress.

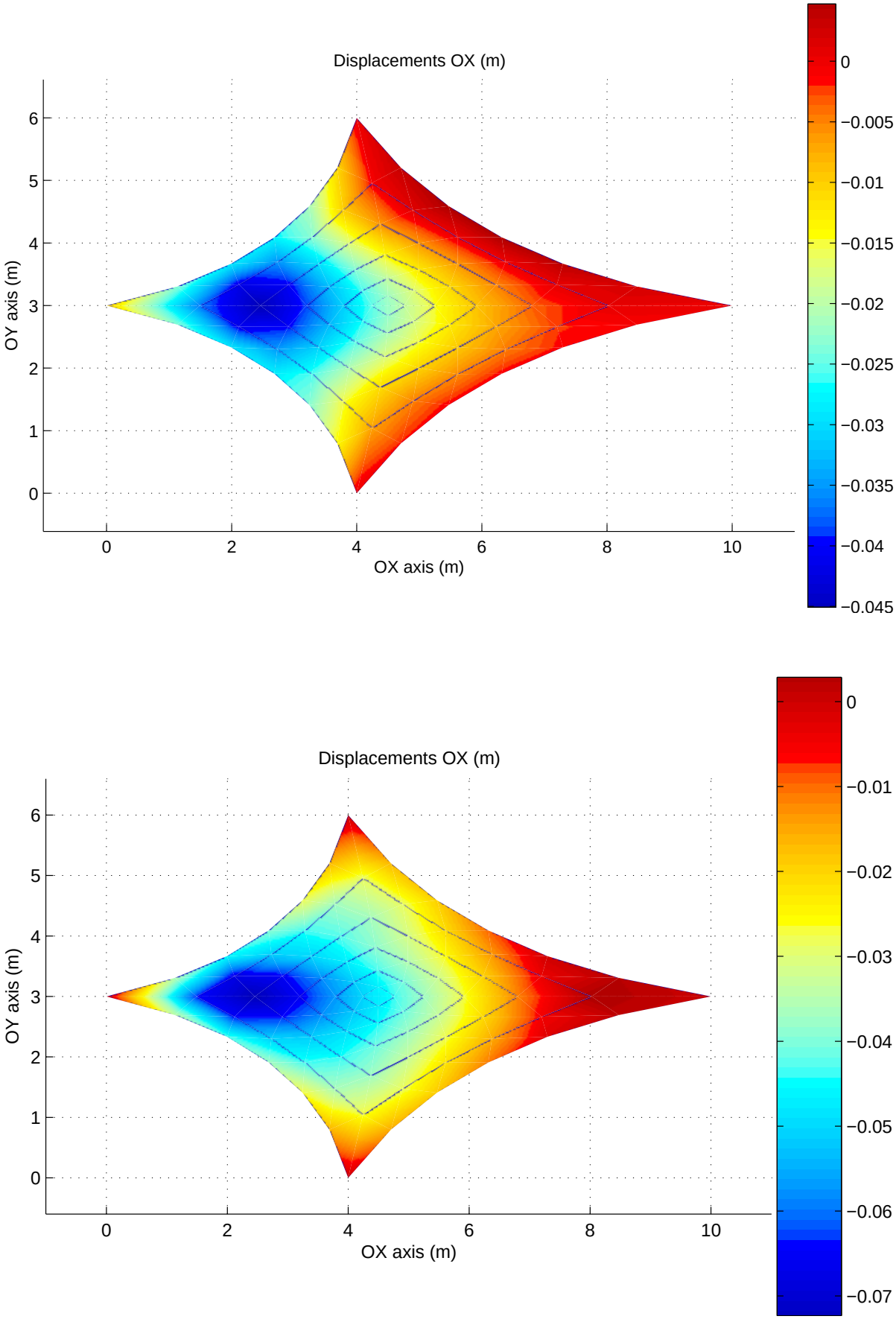

Figure 3.10: Example 1: Displacement plot OX - 1. Prestress stage 2. Snow load

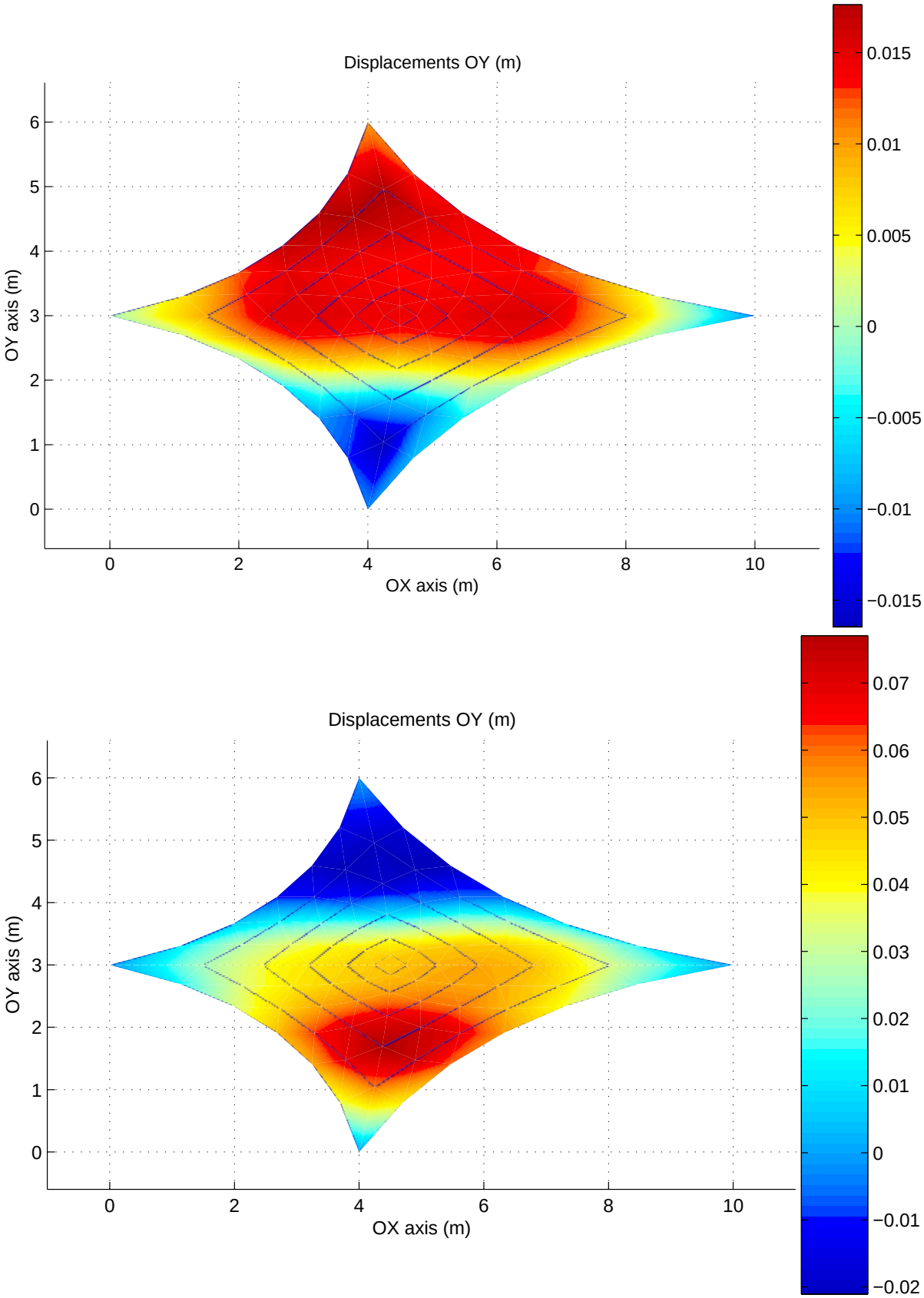

Figure 3.11: Example 1: Displacement plot OY - 1. Prestress stage 2. Snow load

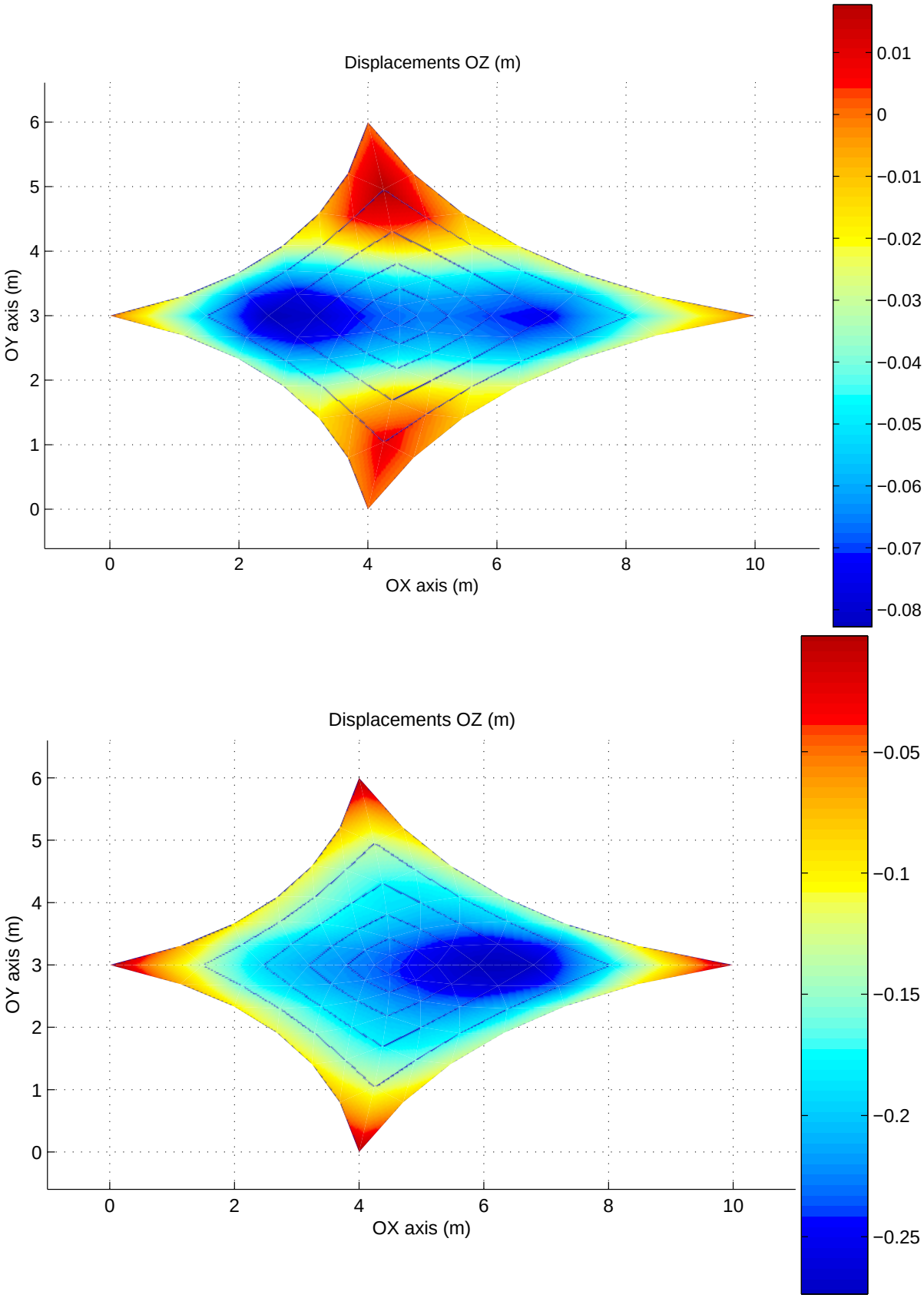

Figure 3.12: Example 1: Displacement plot OZ - 1. Prestress stage 2. Snow load

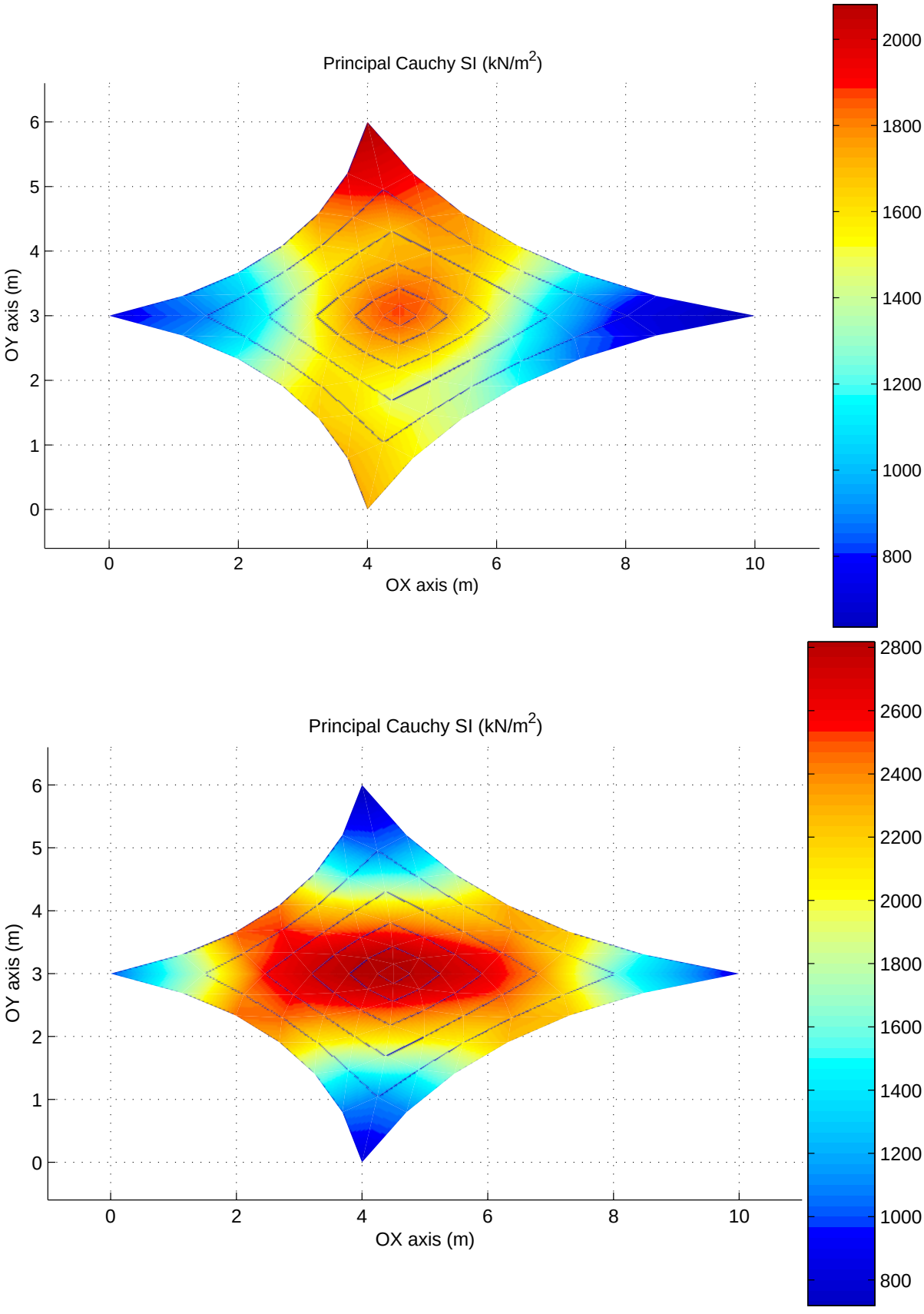

Figure 3.13: Example 1: Principal Cauchy stress σ_1 - 1. Prestress stage 2. Snow load

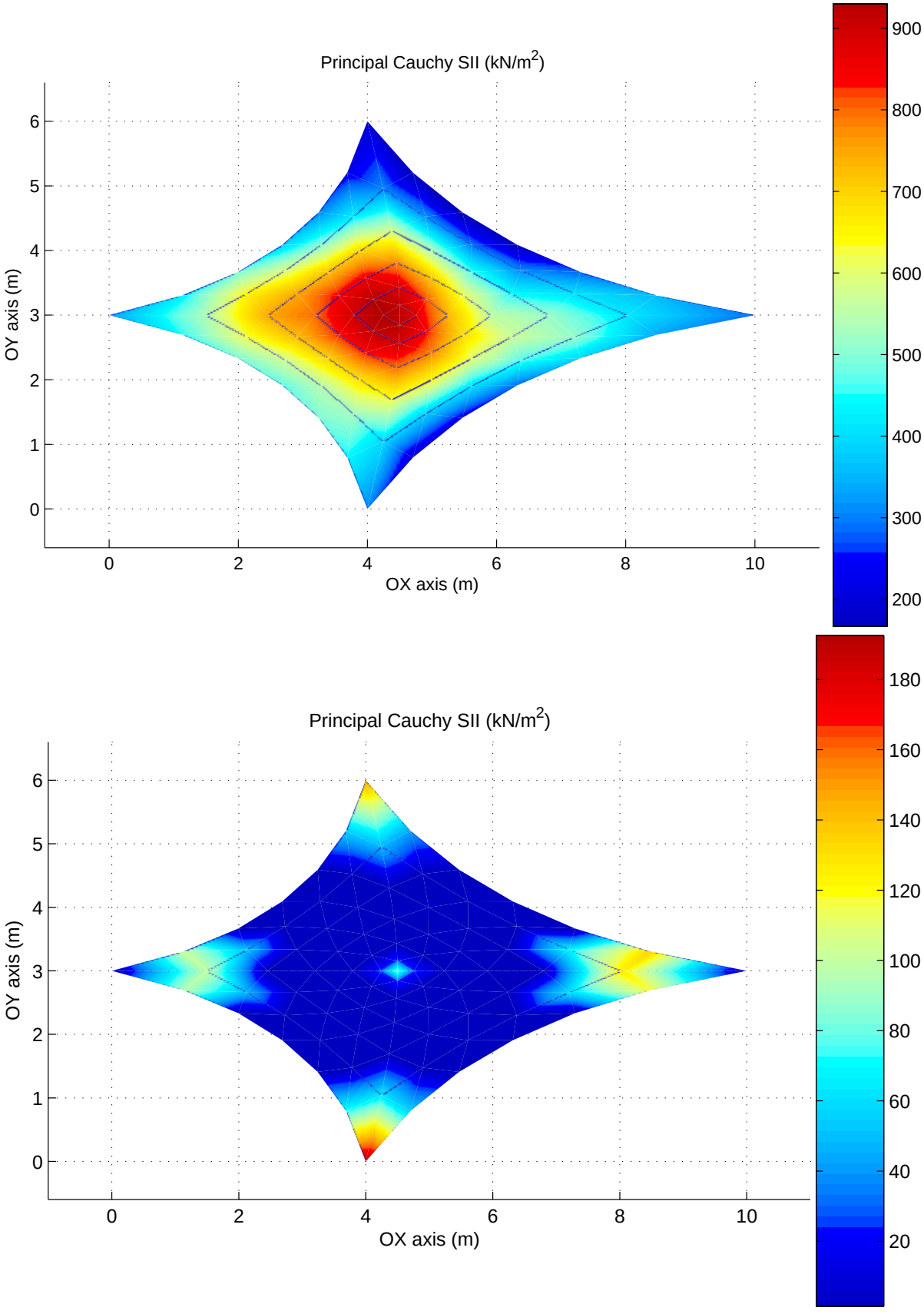

Figure 3.14: Example 1: Principal Cauchy stress σ_{11} - 1. Prestress stage 2. Snow load

Chapter 4

Membrane Bending Formulation

4.1 Introduction

Among the wide variety of tension structures in Architecture and Civil Engineering, both prestressed membranes and cable networks constitute a very remarkable group.These structures are achieving an increasing acceptance level in our society, for example, because of their aesthetic qualities and speed of erection.A large number of tensioned membranes are reinforced by means of interior and perimeter cables. Thus, the analysis of cable elements can be considered as a previous step for a further and comprehensive study of prestressed membranes. Some References in which the authors has pursued analytical solutions are [25], [32] and [16] and those authors who pursued numerical solution are [32], [30] and [6].

Analogously, throughout the last decades, the state of the art of prestressed membranes shows a broad variety of publications, which might be allocated in three different categories:

1. Basic examples which are analyzed by means of analytical approaches; the strong formulation is solved in domains of simple geometry: see [29], [25], [6] and [32]

2. Membranes which are assimilated to cable networks, whereby orthotropic hyperelastic membranes can be analyzed in a fairly accurate manner. Any of the References mentioned in previous paragraphs are valid examples.

3. The exact continuum approach for large strain non-prestressed membranes is studied in multiple References: [8], [4] and [3]. Recent developments are due Bonet et al. [12], [13] and [11].

The some of the early work on development of rotation free element are from [27], [14], [26], [9], [10] and finally [17].

The aim of this chapter is to summarize the Total Lagrangian Formulation for rotation free element followed by a simple numerical examples.

4.2 Membrane Bending Formulation

Let us consider a membrane whose undeformed middle surface occupies the domain Ω_0 in the Euclidean space $\mathbb{R}^3$ with boundary Γ. At each point of this middle surface a thickness t is defined as the distance (measured along the normal to the membrane surface) between the upper and lower surfaces of the membrane. The thickness is assumed to be constant and considered small in comparison with the other dimension of the membrane. We denote $\mathbf{X}$ and $\mathbf{x}$ as the original and deformed positions, respectively, of a generic point of the membrane. These positions are expressed as a function of the co-ordinates of the associated point on the middle surface. The virtual External work due to moment M and virtual change in the curvature can be expressed in the integral form as,

$$\delta W^{(e)}(\vec{\phi}, \delta\vec{v}) = \int_{\Omega^{(e)}} M^{(e)} \delta k^{(e)} d\Omega \tag{4.1}$$

Where

$$\Omega^{(e)} : \text{Membrane domain} = \frac{1}{3}(\Omega_L + \Omega_R) \tag{4.2}$$

And,
The curvatures and the moment relationship can be expressed in the usual manner,

$$M^{(e)} = \alpha k^{(e)} \quad \text{and} \quad \alpha = \frac{t^3}{12} E \tag{4.3}$$

Where M is the bending moment, α is the flexural rigidity, k is th curvature, t is the thickness of the membrane and E is the Young's modulus. Assuming small strains and

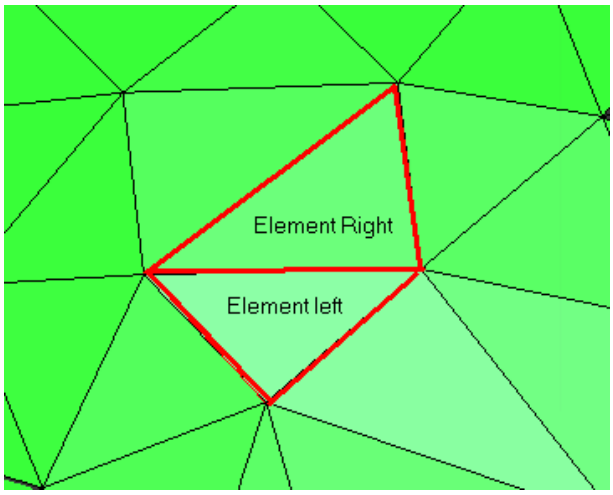

Figure 4.1: Description of Patch for membrane bending calculation

large rotations. The virtual external work can be expressed as,

$$\delta W^{(e)}(\vec{\phi}, \delta\vec{v}) \cong \int_{\Omega_0^{(e)}} M^{(e)} \delta k^{(e)} dV \tag{4.4}$$

where V is the initial volume and Ω_0 is the domain of the patch for the element. The figure 4.1 shows the patch for edge and figure 4.2 shows the domain of the patch for the edge. The domain Ω_0 is taken a $\frac{1}{3}$ of the area of the element to the left and right of the edge as shown. At this stage, it is easier to consider the contribution to $\delta W^{(e)}(\vec{\phi}, \delta\vec{v}^a)$ caused by a single virtual nodal velocity δv_a occurring at a typical node a of element (e). Introducing the interpolation for δv

$$\delta W^{(e)}(\vec{\phi}, N^a \delta\vec{v}^a) \cong \int_{\Omega_0^{(e)}} M^{(e)} \mathbf{D} k^{(e)}(\vec{\phi}) \left[N^a \delta\vec{v}^a\right] dV \tag{4.5}$$

The virtual work per element (e) per node a can, alternatively, be expressed in terms of the internal equivalent nodal forces $T_a^{(e)}$ as,

$$\delta W^{(e)}(\vec{\phi}, N^a \delta\vec{v}^a) = \delta\vec{v}^a \cdot T^a \tag{4.6}$$

Equation 4.6 represents a set of nonlinear equations with the current nodal positions as unknowns. The solution of these equations is achieved using a Newton Raphson iterative procedure that involves the discretization of the linearized equilibrium equations. The virtual external work $\delta W^{(e)}(\vec{\phi}, N^a \delta\vec{v}^a)$ which can be linearized in the direction u to give,

$$\begin{aligned} \mathbf{D}\delta W^{(e)}(\vec{\phi}, N^a \delta\vec{v}^a)[u] \cong & \int_{\Omega_0^{(e)}} \mathbf{D} k^{(e)}(\vec{\phi})[N^a \delta\vec{v}^a] \mathbf{D} M^{(e)}(\vec{\phi})[u] dV \\ & + \int_{\Omega_0^{(e)}} M^{(e)} \mathbf{D}\left[\mathbf{D} k^{(e)}(\vec{\phi})[N^a \delta\vec{v}^a]\right][u] dV \end{aligned} \tag{4.7}$$

Before continuing with the discretization of the linearized equation 4.7. The equation $\delta W^{(e)}(\vec{\phi}, N^a \delta\vec{v}^a) = \delta\vec{v}^a \cdot T^a$ essentially expresses the contribution of the internal nodal

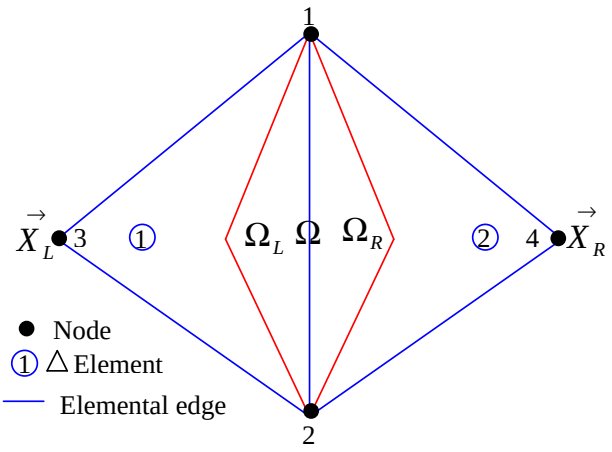

Figure 4.2: Description of domain of the Patch for the edge

equivalent forces $T_a^{(a)}$ at node a. Linearization of equation of internal nodal equivalent forces $T_a^{(a)}$ in the direction $N^b\vec{u}^b$ with $N^a\delta\vec{v}^a$ remaining constant, expresses the change in the internal nodal equivalent forces $T_a^{(a)}$ at node a, due to a change u_b in the current position of node b as,

$$\mathbf{D}\delta W^{(e)}(\vec{\phi}, N^a\delta\vec{v}^a)[N^b\vec{u}^b] \cong \int_{\Omega_0^{(e)}} \mathbf{D}k^{(e)}(\vec{\phi})[N^a\delta\vec{v}^a]\mathbf{D}M^{(e)}(\vec{\phi})[N^b\vec{u}^b]dV + \int_{\Omega_0^{(e)}} M^{(e)}\mathbf{D}\left[\mathbf{D}k^{(e)}(\vec{\phi})[N^a\delta\vec{v}^a]\right][N^b\vec{u}^b]dV \tag{4.8}$$

$$\delta\vec{v}^a \cdot \mathbf{K}_{(e)}^{ab}\vec{u}^b = \int_{\Omega_0^{(e)}} \mathbf{D}k^{(e)}(\vec{\phi})[N^a\delta\vec{v}^a]\alpha\mathbf{D}k^{(e)}(\vec{\phi})[N^b\vec{u}^b]dV + \int_{\Omega_0^{(e)}} M^{(e)}\mathbf{D}\left[\mathbf{D}k^{(e)}(\vec{\phi})[N^a\delta\vec{v}^a]\right][N^b\vec{u}^b]dV \tag{4.9}$$

The relationship between changes in forces at node a due to changes in the current position of node b is furnished by the tangent stiffness matrix $\mathbf{k}_{(e)}^{ab}$, which is clearly seen to derive from the linearization of the virtual work equation. In physical terms the tangent stiffness provides the Newton-Raphson procedure with the operator that adjusts current nodal positions so that the deformation-dependent equivalent nodal forces tend toward being in equilibrium with the external equivalent nodal forces.

To calculate the curvature $k^{(e)}$, the curvature can be expressed as,

$$k^{(e)} = -\frac{\partial\vec{\mathbf{n}}}{\partial S} \cdot \frac{\partial\vec{\mathbf{x}}}{\partial S} \tag{4.10}$$

By using central finite difference approximation, the above equation for curvature can be expressed as,

$$-\frac{\partial\vec{\mathbf{n}}}{\partial S} \cdot \frac{\partial\vec{\mathbf{x}}}{\partial S} \cong -\frac{(\vec{\mathbf{n}}_R - \vec{\mathbf{n}}_L)}{{}^{d_{LR}}_{cg}} \cdot \frac{(\vec{\mathbf{X}}_{cg_R} - \vec{\mathbf{X}}_{cg_L})}{{}^{d_{LR}}_{cg}} \tag{4.11}$$

Where n_R and n_L are the normals of the left and right element in patch. $\vec{\mathbf{X}}_{cg_R}$ and $\vec{\mathbf{X}}_{cg_R}$ are the vector to the centre of gravity of the left and right element of the patch, which is given by,

$$\vec{\mathbf{X}}_{cg_R} - \vec{\mathbf{X}}_{cg_L} = \frac{1}{3}(\vec{\mathbf{X}}_R - \vec{\mathbf{X}}_L) \quad \text{and} \quad {}^{d_{LR}}_{cg} \cong \frac{2}{3L_0^{(e)}}(\Omega_{0_L} + \Omega_{0_R}) \tag{4.12}$$

Where $L_0^{(e)}$ is the initial length of the edge and ${}^{d_{LR}}_{cg}$ is the distance between the cgs of the right and left element of the domain. Substituting for ${}^{d_{LR}}_{cg}$ and $\vec{\mathbf{X}}_{cg}$, we get,

$$k^{(e)} \cong -\frac{(\vec{\mathbf{n}}_R - \vec{\mathbf{n}}_L) \cdot (\vec{\mathbf{X}}_R - \vec{\mathbf{X}}_L)}{3\left[\frac{2}{3L_0^{(e)}}(\Omega_{0_L} + \Omega_{0_R})\right]^2} = \beta\left[\vec{\mathbf{n}}_R \cdot \Delta\vec{\mathbf{X}} - \vec{\mathbf{n}}_L \cdot \Delta\vec{\mathbf{X}}\right] \tag{4.13}$$

Where

$$\beta = \frac{-1}{3\left[\frac{2}{3L_0^{(e)}}(\Omega_{0L} + \Omega_{0R})\right]^2} \quad \text{For small strain} \quad \vec{\mathbf{n}}_R = F_R^{-T}\vec{\mathbf{N}}_R \quad \text{and} \quad \vec{\mathbf{n}}_L = F_L^{-T}\vec{\mathbf{N}}_L \tag{4.14}$$

Where F_R and F_L is the deformation gradient tensor for right and the left element. $\vec{N}_R$ and $\vec{N}_L$ are the normal vector in the initial state. Thus, discretized linear equation of the curvature can be expressed as,

$$\mathbf{D}k^{(e)}(\vec{\phi})[N^a\delta\vec{v}^a] = \beta\left\{\mathbf{D}(\Delta\vec{\mathbf{X}}\cdot F_R^{-T}\vec{\mathbf{N}}_R - \Delta\vec{\mathbf{X}}\cdot F_L^{-T}\vec{\mathbf{N}}_L)[N^a\delta\vec{v}^a]\right\} \tag{4.15}$$

Let us compute, $\mathbf{D}(\Delta\vec{\mathbf{X}}\cdot F^{-T}\vec{\mathbf{N}})[N^a\delta\vec{v}^a]$
Representing in the indicial notation,

$$\mathbf{D}(\Delta\vec{\mathbf{X}}\cdot F^{-T}\vec{\mathbf{N}})[N^a\delta\vec{v}^a] = \mathbf{D}(\Delta\vec{\mathbf{X}}_j\mathbf{N}_k F_{kj}^{-1})[\delta v_i] = \Delta\vec{\mathbf{X}}_j\mathbf{N}_k\mathbf{D}(F_{kj}^{-1})[\delta v_i] \tag{4.16}$$

We know that,

$$\mathbf{D}F^{-1}[\delta\vec{u}] = -F^{-1}\mathbf{D}F[\delta\vec{u}]F^{-1} = -F^{-1}\nabla_0\delta\vec{u}F^{-1} \tag{4.17}$$

For more details see [5]
So,

$$\mathbf{D}(\Delta\vec{\mathbf{X}}\cdot F^{-T}\vec{\mathbf{N}})[N^a\delta v^a] = -\Delta\vec{\mathbf{X}}_j\,\mathbf{N}_k\,F_{ki}^{-1}\,\delta v_i^a\,\nabla_0\mathbf{N}_l^a\,F_{lj}^{-1} = \delta\vec{v^a}\cdot(-\Delta\vec{\mathbf{X}}\cdot F^{-T}\nabla_0\vec{\mathbf{N}}^a)F^{-T}\vec{\mathbf{N}} \tag{4.18}$$

Therefore,the discretized linear equation for the curvature can be expressed as,

$$\begin{aligned}\mathbf{D}k^{(e)}(\vec{\phi})[N^a\delta\vec{v}^a] = \delta\vec{v^a}\cdot\left\{\beta(-\Delta\vec{\mathbf{X}}\cdot F_R^{-T}\nabla_{0R}\vec{\mathbf{N}}^a)F_R^{-T}\vec{\mathbf{N}}_R\right\}\\ -\delta\vec{v^a}\cdot\left\{\beta(-\Delta\vec{\mathbf{X}}\cdot F_L^{-T}\nabla_{0L}\vec{\mathbf{N}}^a)F_L^{-T}\vec{\mathbf{N}}_L\right\}\end{aligned} \tag{4.19}$$

Thus,

$$\begin{aligned}\mathbf{D}k^{(e)}(\vec{\phi})[N^a\delta\vec{v}^a] = \delta\vec{v^a}\cdot\left\{\beta(\Delta\vec{\mathbf{X}}\cdot F_L^{-T}\nabla_{0L}\vec{\mathbf{N}}^a)F_L^{-T}\vec{\mathbf{N}}_L\right\}\\ -\delta\vec{v^a}\cdot\left\{\beta(\Delta\vec{\mathbf{X}}\cdot F_R^{-T}\nabla_{0R}\vec{\mathbf{N}}^a)F_R^{-T}\vec{\mathbf{N}}_R\right\}\end{aligned} \tag{4.20}$$

if node $a \notin$ Left triangle of the patch $\Rightarrow \vec{\nabla}_{0L}\mathbf{N}^a = \vec{\emptyset}$ and if node $a \notin$ Right triangle of the patch as define above $\Rightarrow \vec{\nabla}_{0R}\mathbf{N}^a = \vec{\emptyset}$
The virtual external work can be expressed as,

$$\delta W^{(e)}(\vec{\phi}, N^a\delta\vec{v^a}) \cong \Omega_0^{(e)}M^{(e)}\mathbf{D}k^{(e)}(\vec{\phi})[\vec{N^a}\delta\vec{v^a}] = \Omega_0^{(e)}\alpha k^{(e)}\mathbf{D}k^{(e)}(\vec{\phi})[\vec{N^a}\delta\vec{v^a}] \tag{4.21}$$

$$\text{Where} \qquad \Omega_0^{(e)} = \frac{1}{3}(\Omega_{0L} + \Omega_{0R}) \tag{4.22}$$

$$= \frac{(\Omega_{0_L} + \Omega_{0_R})}{3} \alpha k^{(e)} \delta\vec{v}^a \cdot \left\{ \beta(-\Delta\vec{\mathbf{X}} \cdot F_R^{-T} \nabla_{0R} \vec{\mathbf{N}}^a) F_R^{-T} \vec{\mathbf{N}}_R \right\}$$
$$- \frac{(\Omega_{0_L} + \Omega_{0_R})}{3} \alpha k^{(e)} \delta\vec{v}^a \cdot \left\{ \beta(-\Delta\vec{\mathbf{X}} \cdot F_L^{-T} \nabla_{0L} \vec{\mathbf{N}}^a) F_L^{-T} \vec{\mathbf{N}}_L \right\} \tag{4.23}$$

$$= \delta\vec{v}^a \cdot \underbrace{\left\{ \alpha\, \beta\, \Omega_0^e\, k^{(e)}\, [(\Delta\vec{\mathbf{X}} \cdot F_L^{-T} \nabla_{0L} \vec{\mathbf{N}}^a) F_L^{-T} \vec{\mathbf{N}}_L - (\Delta\vec{\mathbf{X}} \cdot F_R^{-T} \nabla_{0R} \vec{\mathbf{N}}^a) F_R^{-T} \vec{\mathbf{N}}_R] \right\}}_{T^{a(e)}} \tag{4.24}$$

Thus, Equivalent internal nodal force at node a is given by,

$$T^{a(e)} = \alpha\, \beta\, \Omega_0^e\, k^{(e)}\, [(\Delta\vec{\mathbf{X}} \cdot F_L^{-T} \nabla_{0L} \vec{\mathbf{N}}^a) F_L^{-T} \vec{\mathbf{N}}_L - (\Delta\vec{\mathbf{X}} \cdot F_R^{-T} \nabla_{0R} \vec{\mathbf{N}}^a) F_R^{-T} \vec{\mathbf{N}}_R] \tag{4.25}$$

Where

$$k^{(e)} \cong \beta \Delta\vec{\mathbf{X}} \cdot (F_R^{-T} \vec{\mathbf{N}}_R - F_L^{-T} \vec{\mathbf{N}}_L) \qquad \beta = \frac{-3(L_0^{(e)})^2}{4(\Omega_{0_L} + \Omega_{0_R})} \tag{4.26}$$

$$\text{and} \qquad \Omega_0^{(e)} = \frac{1}{3}(\Omega_{0_L} + \Omega_{0_R}) \tag{4.27}$$

The first part of the equation 4.9 which is called as Constitutive stiffness matrix can be expressed as,

$$\mathbf{D}^c \delta W(\vec{\phi}, N^a \delta\vec{v}^a)[N^b \vec{u}^b] \cong \Omega_0^{(e)}\, \alpha\, \mathbf{D}k^{(e)}(\vec{\phi})\, [N^a \delta\vec{v}^a]\, \mathbf{D}k^{(e)}(\vec{\phi})[N^b \vec{u}^b] \tag{4.28}$$

$$= \Omega_0^{(e)}\, \alpha\, \delta\vec{v}^a \cdot \vec{S}^a \otimes \vec{S}^b\, \vec{u}^b = \delta\vec{v}^a \cdot (\Omega_0^{(e)}\, \alpha\, \vec{S}^a \otimes \vec{S}^b)\, \vec{u}^b \tag{4.29}$$

Where

$$\vec{S}^a = \beta[(\Delta\vec{\mathbf{X}} \cdot F_L^{-T} \nabla_{0L} \vec{N}^a) F_L^{-T} \vec{N}_L - (\Delta\vec{\mathbf{X}} \cdot F_R^{-T} \nabla_{0R} \vec{N}^a) F_R^{-T} \vec{N}_R] \tag{4.30}$$

Finally the Constitutive part of the stiffness matrix can be written as,

$$\mathbf{K}^{c,ab(e)} = \Omega_0^{(e)} \alpha\, \vec{S}^a \otimes \vec{S}^b \tag{4.31}$$

To simplify the representation, we can define,

$$\vec{G}^a = (\Delta\vec{\mathbf{X}} \cdot F^{-T} \nabla_0 \vec{N}^a)\, F^{-T} \vec{\mathbf{N}} \tag{4.32}$$

Discretizing the linearined equation for $\vec{G}^a$ in the direction u, representing in the indicial notation,

$$\mathbf{D}\vec{G}^a[\vec{N}^b \vec{u}^b] = \mathbf{D}(\Delta\mathbf{X}_m\, F_{lm}^{-1}\, \nabla_0\, N_l^a\, F_{ki}^{-1}\, \mathbf{N}_k)\, [u_j] \tag{4.33}$$

$$= \Delta\mathbf{X}_m\, \mathbf{D}(F_{lm}^{-1})[u_j]\, \nabla_0 N_l^a\, F_{ki}^{-1}\, \mathbf{N}_k$$
$$+ \Delta\mathbf{X}_m\, F_{lm}^{-1}\, \nabla_0 N_l^a\, \mathbf{N}_k\, \mathbf{D}(F_{ki}^{-1})[u_j] \tag{4.34}$$

But linearizing F_{lm}^{-1} and F_{ki}^{-1} along u

$$\mathbf{D}(F_{lm}^{-1})[u_j] = -F_{lj}^{-1} u_j^b \nabla_0 N_n^b F_{nm}^{-1} \quad \text{and}\, \mathbf{D}(F_{ki}^{-1})[u_j] = -F_{kj}^{-1} u_j^b \nabla_0 N_n^b F_{ni}^{-1} \tag{4.35}$$

Substituting for above terms, we get

$$\begin{aligned} &= (-\nabla_0 N_n^b F_{nm}^{-1} \Delta \mathbf{X}_m)(F_{ki}^{-1} N_k)(\nabla_0 N_l^a F_{lj}^{-1})\, u_j^b \\ &+ (-\nabla_0 N_l^a F_{lm}^{-1} \Delta \mathbf{X}_m)(F_{ni}^{-1} \nabla_0 N_n^b)(F_{kj}^{-1} N_k)\, u_j^b \end{aligned} \tag{4.36}$$

$$\begin{aligned} &= (-\Delta \vec{\mathbf{X}} \cdot F^{-T} \nabla_0 \vec{N}^b)\, (F^{-T} \vec{\mathbf{N}}) \otimes (F^{-T} \nabla_0 \vec{N}^a)\, \vec{u}^b \\ &+ (-\Delta \vec{\mathbf{X}} \cdot F^{-T} \nabla_0 \vec{N}^a)\, (F^{-T} \nabla_0 \vec{N}^b) \otimes (F^{-T} \vec{\mathbf{N}})\, \vec{u}^b \end{aligned} \tag{4.37}$$

The second part of the equation 4.9 is the Geometric stiffness matrix, which can be expressed as,

$$\mathbf{D}^m \delta W^{(e)}(\vec{\phi}, N^a \delta \vec{u}^a)[N^b \vec{u}^b] \cong \Omega_0^{(e)} \alpha k^{(e)} \mathbf{D}(\delta \vec{v}^a \cdot (\beta \vec{G}_L^a - \beta \vec{G}_R^a))\, [N^b \vec{u}^b] \tag{4.38}$$

$$= \Omega_0^{(e)}\, M^{(e)}\, \beta\, \delta \vec{v}^a \cdot \left\{ \mathbf{D}\vec{G}_L^a [N^b \vec{u}^b] - \mathbf{D}\vec{G}_R^a [N^b \vec{u}^b] \right\} \tag{4.39}$$

Linearizing and Substituting for $\vec{G}^a$ into above equation we get,

$$\begin{aligned} \mathbf{D}\vec{G}_L^a [N^b \vec{u}^b] &= (-\Delta \vec{\mathbf{X}} \cdot F_L^{-T} \nabla_{0L} \vec{N}^b)\, (F_L^{-T} \vec{\mathbf{N}}_L) \otimes (F_L^{-T} \nabla_{0L} \vec{N}^a)\, \vec{u}^b \\ &+ (-\Delta \vec{\mathbf{X}} \cdot F_L^{-T} \nabla_{0L} \vec{N}^a)\, (F_L^{-T} \nabla_{0L} \vec{N}^b) \otimes (F_L^{-T} \vec{\mathbf{N}}_L) \vec{u}^b \end{aligned} \tag{4.40}$$

$$\begin{aligned} \mathbf{D}\vec{G}_R^a [N^b \vec{u}^b] &= (-\Delta \vec{\mathbf{X}} \cdot F_R^{-T} \nabla_{0R} \vec{N}^b)\, (F_R^{-T} \vec{\mathbf{N}}_R) \otimes (F_R^{-T} \nabla_{0R} \vec{N}^a)\, \vec{u}^b \\ &+ (-\Delta \vec{\mathbf{X}} \cdot F_R^{-T} \nabla_{0R} \vec{N}^a)\, (F_R^{-T} \nabla_{0R} \vec{N}^b) \otimes (F_R^{-T} \vec{\mathbf{N}}_R)\, \vec{u}^b \end{aligned} \tag{4.41}$$

Thus, Geometric stiffness matrix can be expressed as,

$$\begin{aligned} \mathbf{K}^{m_{ab}^{(e)}} &= \Omega_0^{(e)} M^{(e)} \beta (\Delta \vec{\mathbf{X}} \cdot F_R^{-T} \nabla_{0R} \vec{N}^b)(F_R^{-T} \vec{\mathbf{N}}_R) \otimes (F_R^{-T} \nabla_{0R} \vec{N}^a) \\ &+ \Omega_0^{(e)} M^{(e)} \beta (\Delta \vec{\mathbf{X}} \cdot F_R^{-T} \nabla_{0R} \vec{N}^a)(F_R^{-T} \nabla_{0R} \vec{N}^b) \otimes (F_R^{-T} \vec{\mathbf{N}}_R) \\ &- \Omega_0^{(e)} M^{(e)} \beta (\Delta \vec{\mathbf{X}} \cdot F_L^{-T} \nabla_{0L} \vec{N}^b)(F_L^{-T} \vec{\mathbf{N}}_L) \otimes (F_L^{-T} \nabla_{0L} \vec{N}^a) \\ &- \Omega_0^{(e)} M^{(e)} \beta (\Delta \vec{\mathbf{X}} \cdot F_L^{-T} \nabla_{0L} \vec{N}^a)(F_L^{-T} \nabla_{0L} \vec{N}^b) \otimes (F_L^{-T} \vec{\mathbf{N}}_L) \end{aligned} \tag{4.42}$$

To simplify the notation, define

$$P_R^a = (\Delta \vec{\mathbf{X}} \cdot F_R^{-T} \nabla_{0R} \vec{N}^a) \quad \text{(analogously for } P_R^b, P_L^a, P_L^b) \tag{4.43}$$

$$\vec{S}_R = F_R^{-T} \vec{\mathbf{N}}_R \quad \text{(analogously for } \vec{S}_L) \tag{4.44}$$

$$\vec{t}_R^a = F_R^{-T} \nabla_{0R} \vec{N}^a \quad \text{(analogously for } \vec{t}_R^b, \vec{t}_L^a, \vec{t}_L^b) \tag{4.45}$$

Thus substituting the above notation, We have the curvature as,

$$k^{(e)} = \beta\, \Delta \vec{\mathbf{X}} \cdot (\vec{S}_R - \vec{S}_L) \tag{4.46}$$

Moment is given by,

$$M^{(e)} = \alpha\, k^{(e)} \tag{4.47}$$

The equivalent nodal forces is given

$$T_a^{(e)} = \Omega_0^{(e)} M^{(e)} \beta \left(P_L^a \, \vec{S}_L - P_R^a \, \vec{S}_R \right) \tag{4.48}$$

The constitutive part of the element stiffness matrix due to bending is given,

$$\mathbf{K}^{c_{ab}^{(e)}} = \Omega_0^{(e)} \alpha \, \beta^2 \left[P_L^a \, \vec{S}_L - P_R^a \, \vec{S}_R \right] \otimes \left[P_L^b \, \vec{S}_L - P_R^b \, \vec{S}_R \right] \tag{4.49}$$

The geometric part of the element stiffness matrix due to bending is given,

$$\mathbf{K}^{m_{ab}^{(e)}} = \Omega_0^{(e)} M^{(e)} \beta \left\{ P_R^b \, \vec{S}_R \otimes \vec{t}_R^{\,a} + P_R^a \, \vec{t}_R^{\,b} \otimes \vec{S}_R - P_L^b \, \vec{S}_L \otimes \vec{t}_L^{\,a} + P_L^a \, \vec{t}_L^{\,b} \otimes \vec{S}_L \right\} \tag{4.50}$$

4.3 Numerical Results

To illustrate and validate the developed solution process for membrane bending finite element, different numerical examples will be analyzed in detail. Some numerical results will be checked with the ones reported in the existing literature to conclude the validity and quality of the methods used herein. An attempt will be made to prove the quadratic convergence of the Newton-Raphson scheme.

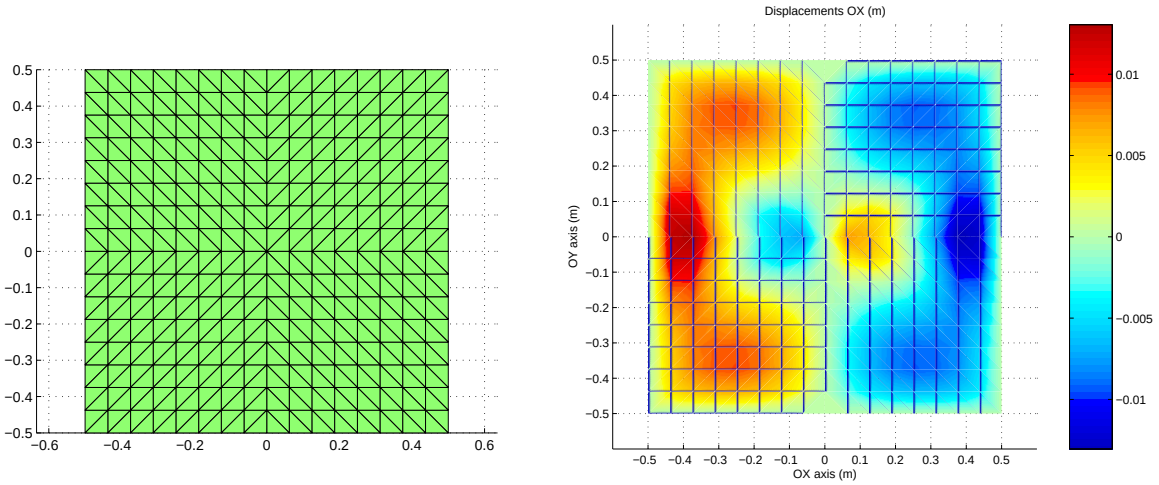

Figure 4.3: Description of the Mesh and Displacement in x-direction

4.3.1 Example 1

This first example is the problem of laterally uniformly loaded initially plane square membrane without any prestress. This is a general problem used to check the stability of the solution. The dimensions of the square membrane are 1m x 1m side and thickness 0.169 m was considered. A isotropic material with Young's modulus $E = 5.8637 kN/m^2$ and the Poisson's ratio $\nu = 0.3$ was considered. The geometry was discretized with linear triangular elements(512 Elements). The boundaries of the square membrane was clamped. A

uniform load intensity of $q = 0.02096kN/m^2$ was applied perpendicularly downward on to the plane. The figure 4.3 shows discretization of the geometry.

As a first step, the problem was analysed with only membrane element without any bending formulation. As discussed earlier since for a pure membrane element the tangent stiffness component along thickness is zero. This will lead to high instability in the analysis as the matrix become singular. This was observed when the problem was analysed with only membrane element without bending.

In the second step the problem was analysed with bending. Since due to the bending

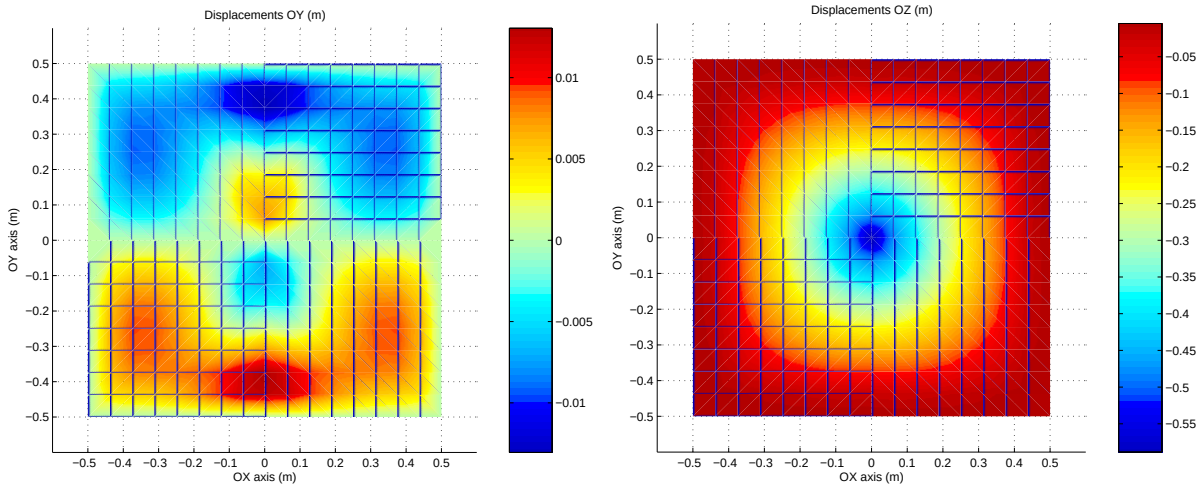

Figure 4.4: Displacement in y-direction and z direction

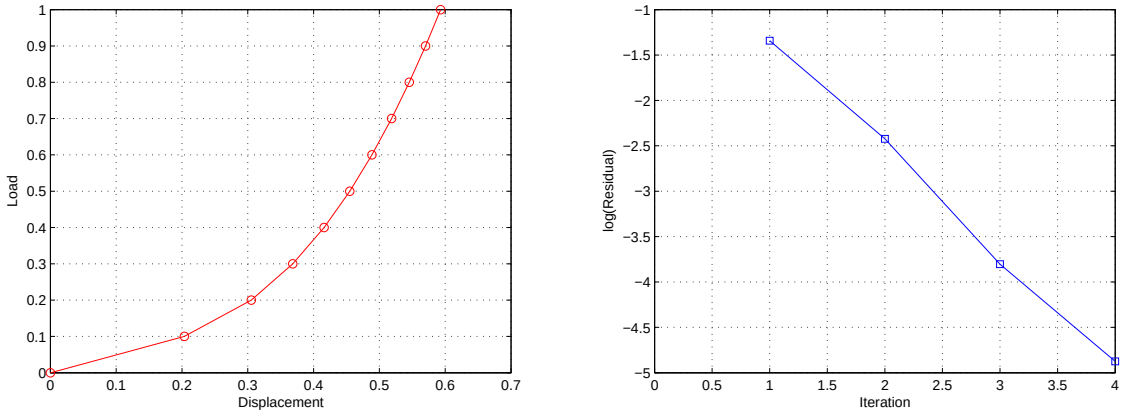

Figure 4.5: Load-deflection curve$(m, \frac{kN}{m^2})$ and Convergence curve

stiffness being added, the analysis should converge without any instability. The first order methods along with the Newton-Rapson method was used to analysed the problem. The problem was analysed in ten equal load increments to get the variation of the displacement with respect to load. The figure 4.5 shows the displacement curve and convergence curve for the last increment. Figure 4.3 and figure 4.4 shows the displacements in x, y and z

direction.

It can conclude from this example the bending formulation has indeed added stiffness component in the third direction, which has help the analysis to complete without any instability whatsoever. The convergence is nearly quadratic showing the well implementation of the Newton-Rapson algorithm.

4.3.2 Example 2

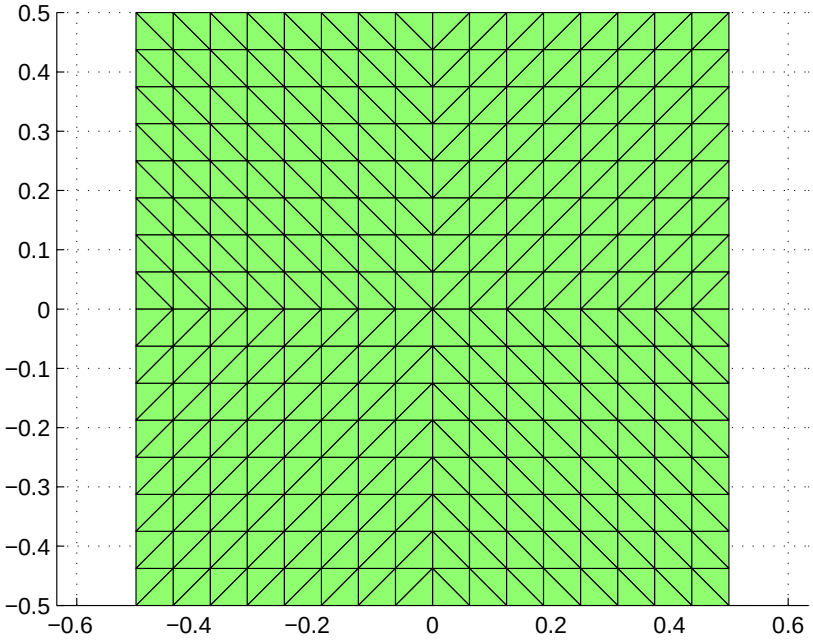

Figure 4.6: Description of the Mesh - Total 1536 dof , 512 Elements

In the example 1 it was shown that the pure membrane which has a zero stiffness component along third direction, will lead to severe instability in the analysis. To overcome this problem Levenberg-Marquardt method can be used. In this method the total tangent stiffness matrix is modified by adding a small value to the diagonal elements of the tangent stiffness matrix. This modification can be viewed as adding a fictitious prestress to the problem. Usually this method is adapted only for few initial iterations of the analysis with very small value. Since this methods does not added any bending stiffness to the problem, it provides a good means to compare the analysis by adding bending stiffness.

It is a laterally uniformly loaded initially plane square membrane without any prestress. The dimensions of square membrane are 1m x 1m side and thickness of 0.169 m was considered. A isotropic material with Young's modulus $E = 5.8637kN/m^2$ and the Poisson's ratio $\nu = 0.3$ was considered. The geometry was discretized with linear triangular elements (512 Elements). The boundaries of the square membrane was clamped. A

uniform load intensity of $q = 0.02096kN/m^2$ was applied perpendicularly downward on to the plane. The figure 4.6 shows discretization of the geometry.

As a first step, the problem was analysed with only membrane elements with

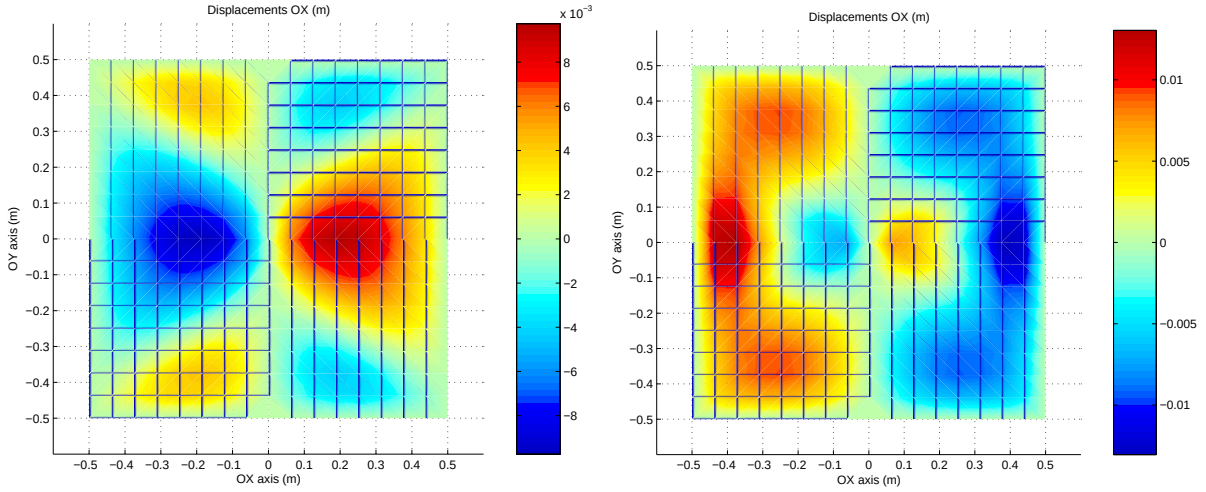

Figure 4.7: Example 2: Displacement in x-direction 1. Without Bending, 2. With Bending

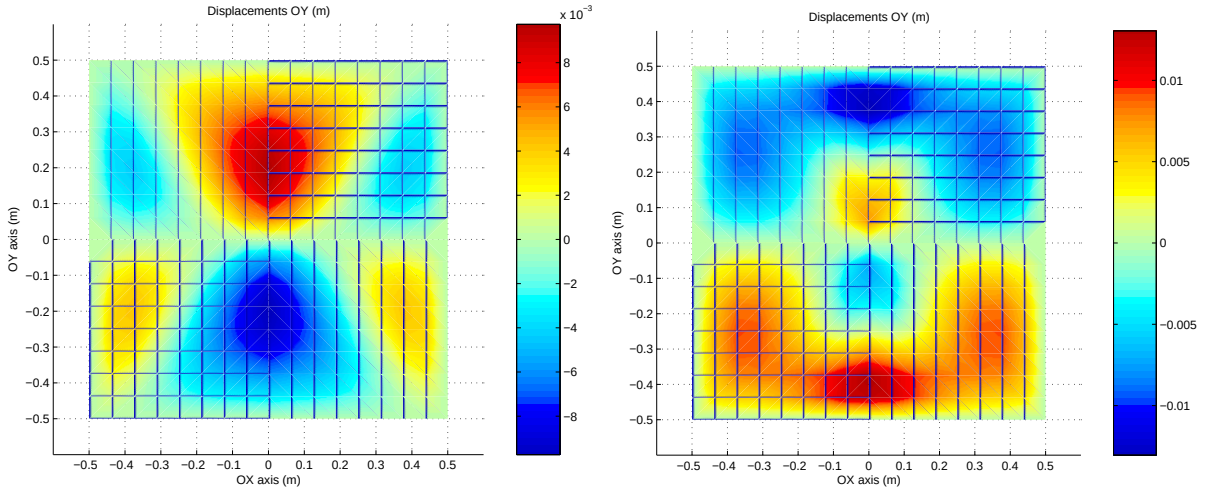

Figure 4.8: Example 2: Displacement in y-direction 1. Without Bending, 2. With Bending

Levenberg-Marquardt method without any bending stiffness. The Levenberg-Marquardt method was adapted for very few initial iterations in the analysis. As a second step, the problem was analysed with bending formulation. For both of the analysis, the first order methods along with the Newton-Rapson method was used to analysed the problem. The problem was analysed in ten equal load increments to get the variation of the displacement with respect to load. In both of the analysis, the solution converged without any instability, as expected. The figure 4.7, 4.8 and 4.9 shows the displacement along x, y and z direction for both of the cases. (Note: Without bending means the analysis is run applying Levenberg-Marquardt method). The figure 4.10 shows the load-deflection

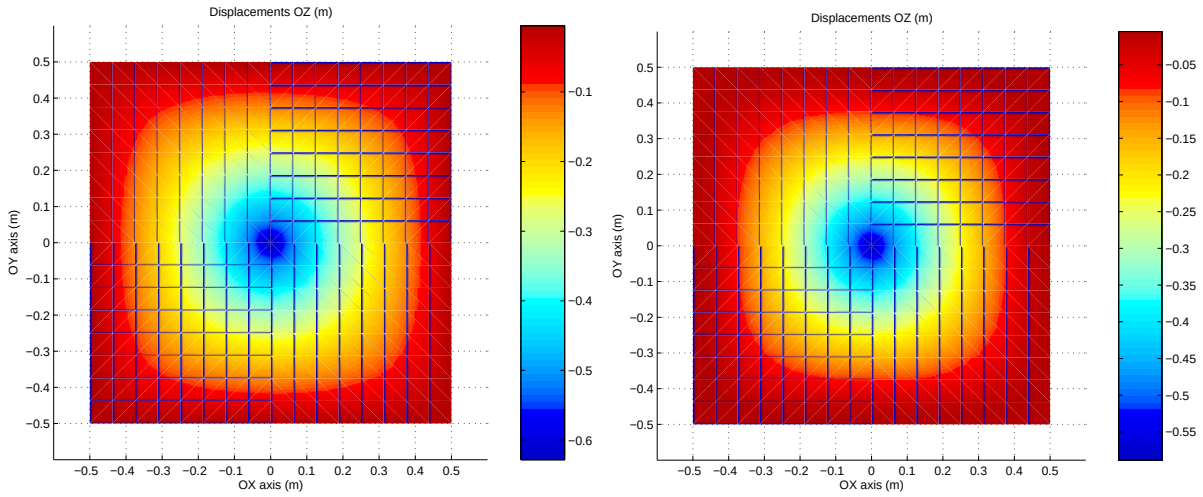

Figure 4.9: Example 2: Displacement in z-direction 1. Without Bending, 2. With Bending

curve for the centrally loaded membrane for both the cases. It can be observed that the displacement in case where Levenberg-Marquardt method is used is more when compared to the case where bending stiffness is added. Figure 4.11 shows the convergence curve for the last increment for both the cases.

It can conclude from this example Levenberg-Marquardt method helps to converge

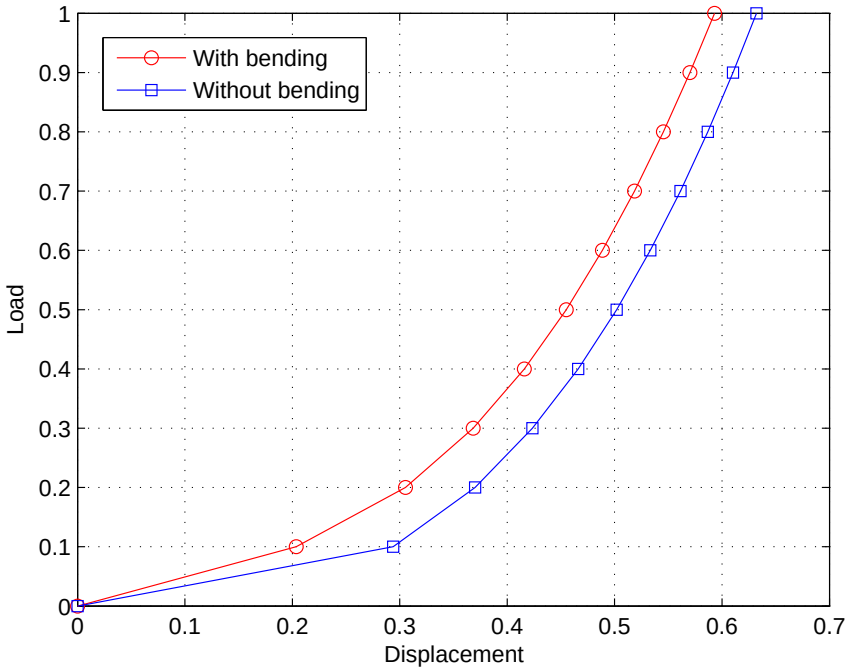

Figure 4.10: Example 2: Load - deflection curve for center of the membrane

to a solution without any instability in the analysis. The solution in first case (applying Levenberg-Marquardt method) can be considered as pure membrane analysis without any

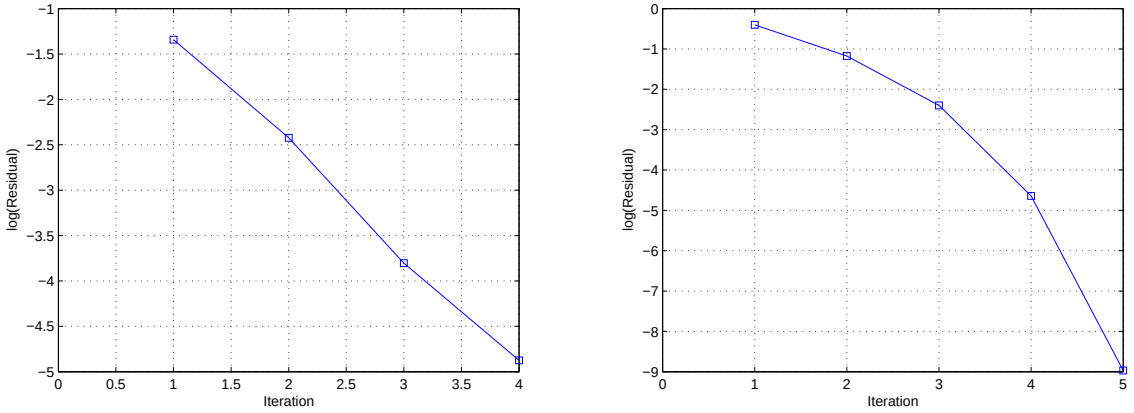

Figure 4.11: Example 2: Convergence curves for 1. Without Bending, 2. With Bending

flexural stiffness, provided that the added values are small and used for initial stability of the solution only. Whereas in the second case, the analysis is carried out by accounting for the change in the internal force and tangent stiffness matrix due to bending. As it can be observed the displacement in first case is more than in second case showing the clear effect of bending on the displacement as compared to a pure membrane deflection. The convergence is quadratic in 1st case and is nearly quadratic in the second case showing the well implementation of the Newton-Rapson algorithm.

4.3.3 Example 3

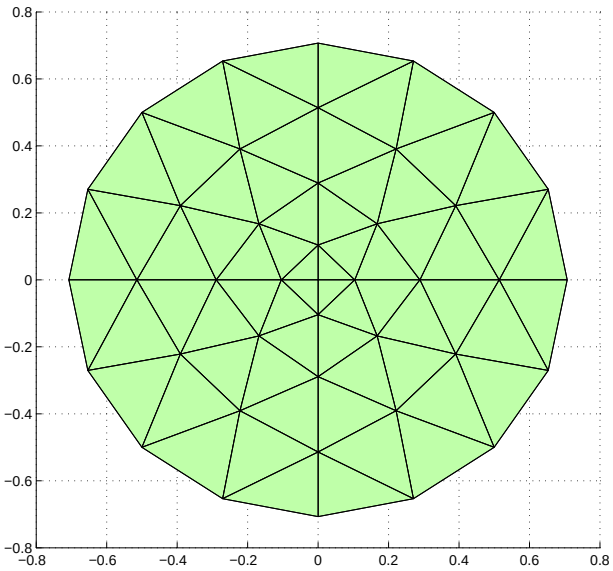

Figure 4.12: Description of the Mesh - Total 196 dof, 64 Elements

This example is drawn from Theory of plates and shells(Timosheko and woinowsky-krieger) see [29] which provide as approximate solution for uniformly loaded circular plate with large deflection. Originally this approximate solution was developed by A.Nadai see [23]. According to this the approximate formulae for deflection of uniformly loaded circular thin plate having large deflection with clamped edge is,

$$\frac{w_0}{h} = 0.583\frac{w_0}{h^3} - 0.176\frac{q}{E}(\frac{a}{h})^4 \tag{4.51}$$

The above formulae is valid for a Poisson's ratio of $\nu = 0.25$
Where, w_0 is the central deflection.
h is the thickness
q is the load intensity
a is the radius of the plate
E is Young's Modulus of the material.

It is laterally uniformly loaded initially plane circular thin plate. The thin plate has

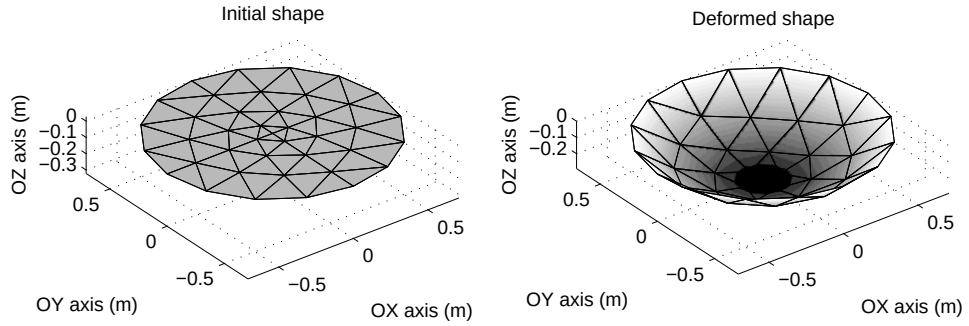

Figure 4.13: Example 3: Undeformed and Deformed shape

radius of $0.7071m$ and thickness of $0.01m$. A isotropic material with Young's modulus $E = 5.8637kN/m^2$ and the Poisson's ratio $\nu = 0.25$ was considered. The geometry was discretized with linear triangular elements (64 Elements). The boundary of the circular plate was clamped. A uniform load intensity of $q = 0.02096kN/m^2$ was applied perpendicularly downward on to the plate. The figure 4.12 shows discretization of the geometry.

For the analysis, the first order methods along with the Newton-Rapson method was used to analysed the problem. The problem was analysed in ten equal load increments to get the variation of the displacement with respect to load. In the analysis the solution converged. The figure 4.13 shows the initial and deformed shape. Figure 4.14 and 4.15 shows the displacement along x, y and z direction.

The figure 4.16 load-deflection curve for the center of the plate. It can be observed that the displacement is Numerical solution is very close to the approximate solution of A.Nadai[23]. Figure 4.17 shows the convergence curve for the first increment.

From the above example it can be concluded that the displacement from the nu-

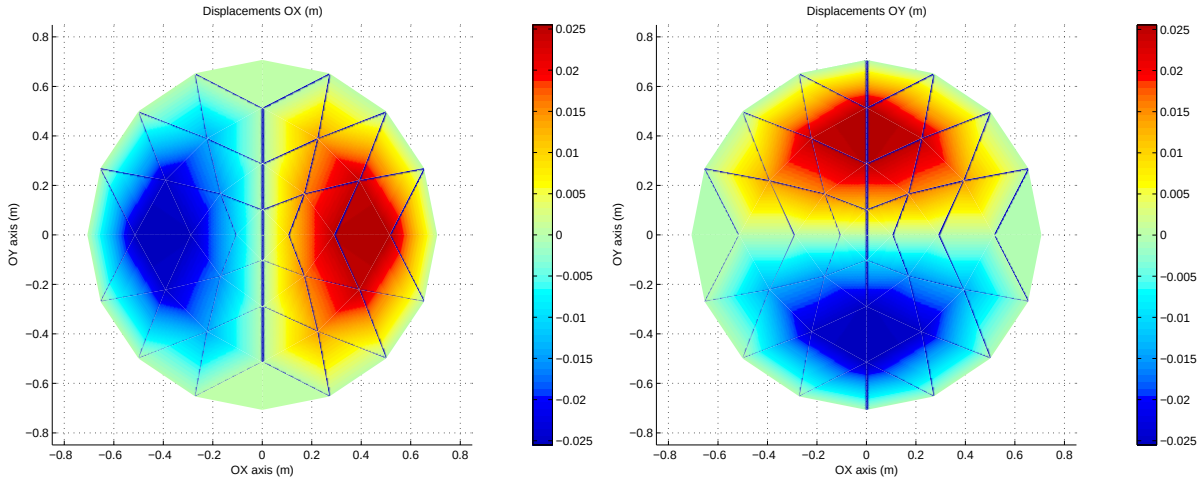

Figure 4.14: Example 2: Displacement in x-direction and y direction

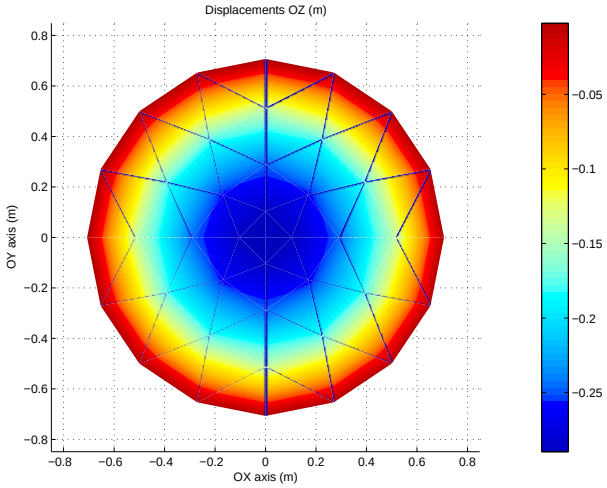

Figure 4.15: Example 3: Displacement in z-direction

merical solution is very close to the approximate solution of A.Nadai[23]. This shows the validity of the present formulation. The convergence curve shows the convergence rate of the first order methods which takes more iteration where for Newton-rapson method it is quadratic.This example shows the over all well implementation of the bending formulation.

4.3.4 Example 4

This example is drawn from Theory of plates and shells (Timosheko and woinowsky-krieger) [29] which provide as approximate solution for uniformly loaded square membrane with large deflection. Calculation for this is provided in book Drang and Zwang [1]. According to this, the approximate formulae for central deflection of uniformly loaded

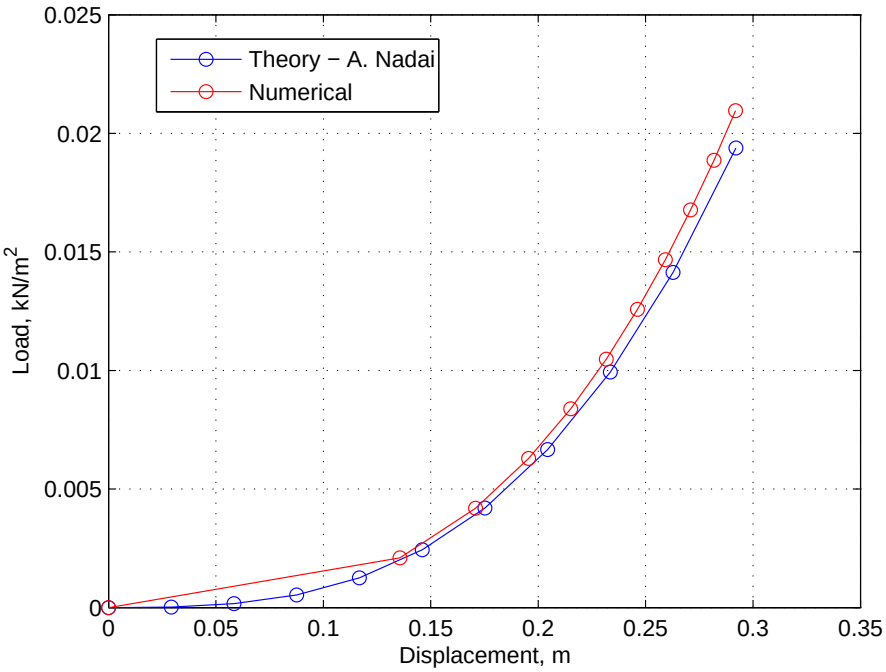

Figure 4.16: Example 3: Load - deflection curve for center of the plate w_0

square membrane having large deflection with clamped edge is,

$$w_0 = 0.802a\sqrt[3]{\frac{qa}{Eh}} \tag{4.52}$$

The above formule is valid for a Poisson's ratio of $\nu = 0.25$ and the solution is assumed to have zero flexural rigidity.
Where, w_0 is the central deflection.
h is the thickness
q is the load intensity
$2a$ is the length of the sides
E is Young's Modulus of the material.

It is a laterally uniformly loaded initially plane square membrane. The membrane dimension are 1m x 1m in sides and thickness of 0.01m was considered. A isotropic material with Young's modulus $E = 5.8637kN/m^2$ and the Poisson's ratio $\nu = 0.25$ was considered. The geometry was discretized with linear triangular elements. The boundaries of the square membrane was clamped. A uniform load intensity of $q = 0.02096kN/m^2$ was applied perpendicularly downward on to the plate. The two different mesh was created to study the convergence. The figure 4.18 shows discretization of the geometry.

For the analysis, the first order methods along with the Newton-Rapson method was used to analysed the problem. The problem was analysed in ten equal load increments to

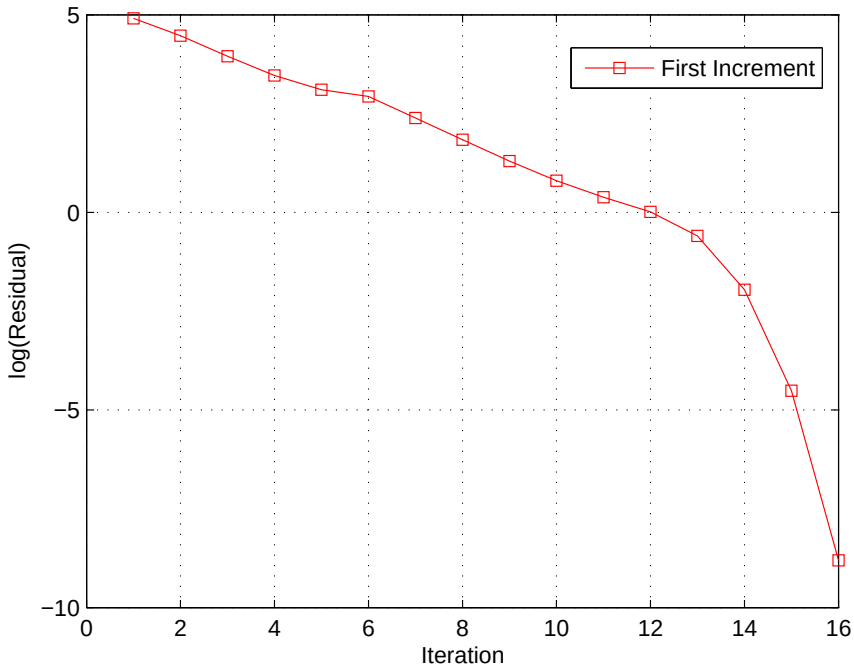

Figure 4.17: Example 3: Convergence curves

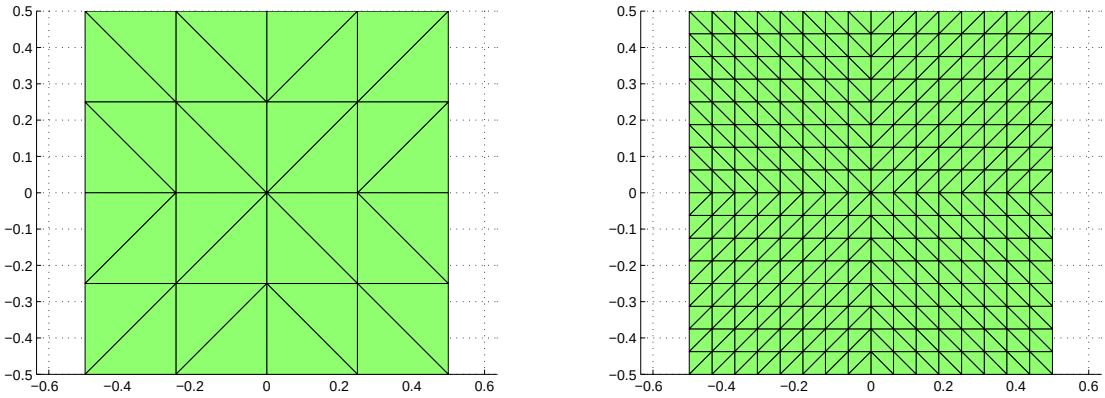

Figure 4.18: Description of the Mesh - Mesh 1: 32 Elemnts, Mesh 2: 512 Elements

get the variation of the displacement with respect to load. In the analysis, the solution converged. The figure 4.19 and figure 4.20 shows the initial and deformed shape for two different mesh. Figure 4.21, figure 4.22 and figure 4.23 shows the displacement along x, y and z direction.

The figure 4.24 load-deflection curve for the center of the plate. It can be observed that the displacement is numerical 1 solution is very close to that of approximate solution of August and Ludwig. It can also be observed that the displacement in numerical 2 is less than that of numerical 1. Figure 4.25 shows the convergence curve for the first increment.

The approximate solution neglects the flexural rigidity and the numerical 1 is dis-

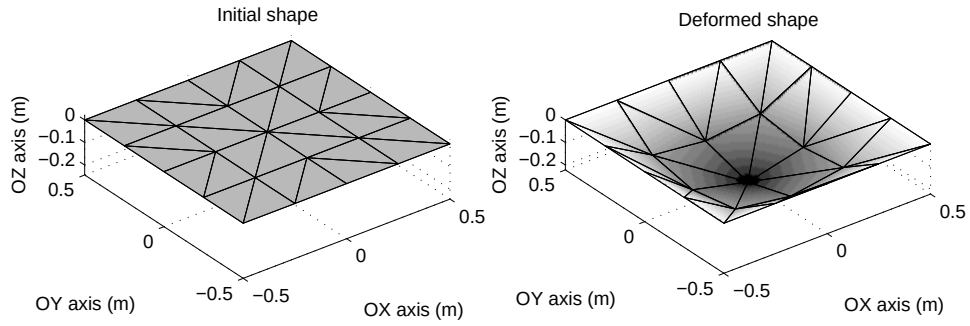

Figure 4.19: Example 4: Undeformed and deformed shape for Numerical 1

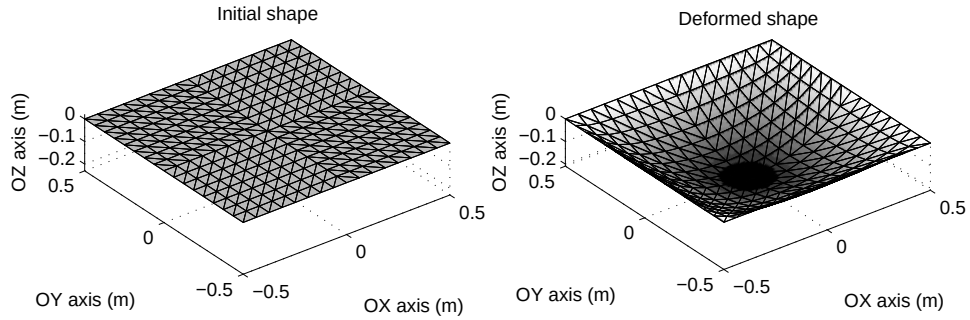

Figure 4.20: Example 4: Undeformed and deformed shape for Numerical 2

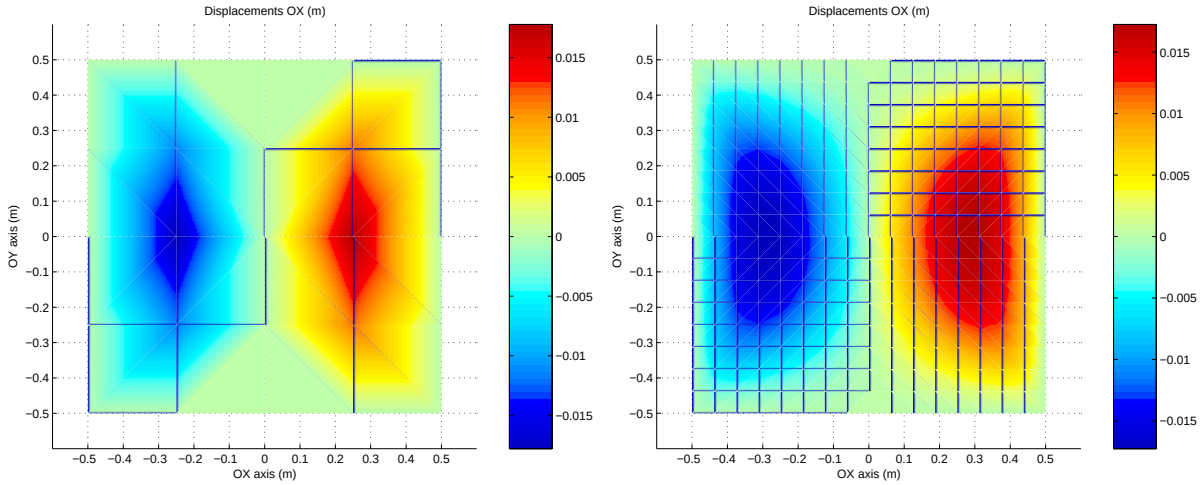

Figure 4.21: Example 4: Displacement in x-direction 1. Numerical 1, 2. Numerical 2

cretized with few elements which contributes less to bending stiffness, this shows the well formulation for bending element. Since in the numerical 1 because of the fewer element the curvature calculation is less accurate, but whereas in the numerical 2 because of the more number of element the curvature calculation is more accurate. It can also be observed that the displacement in case of numerical 2 is less compared to numerical 1 which shows the effect of bending stiffness. The convergence curve shows the convergence rate of the first order methods which takes more iteration whereas, for Newton-rapson method

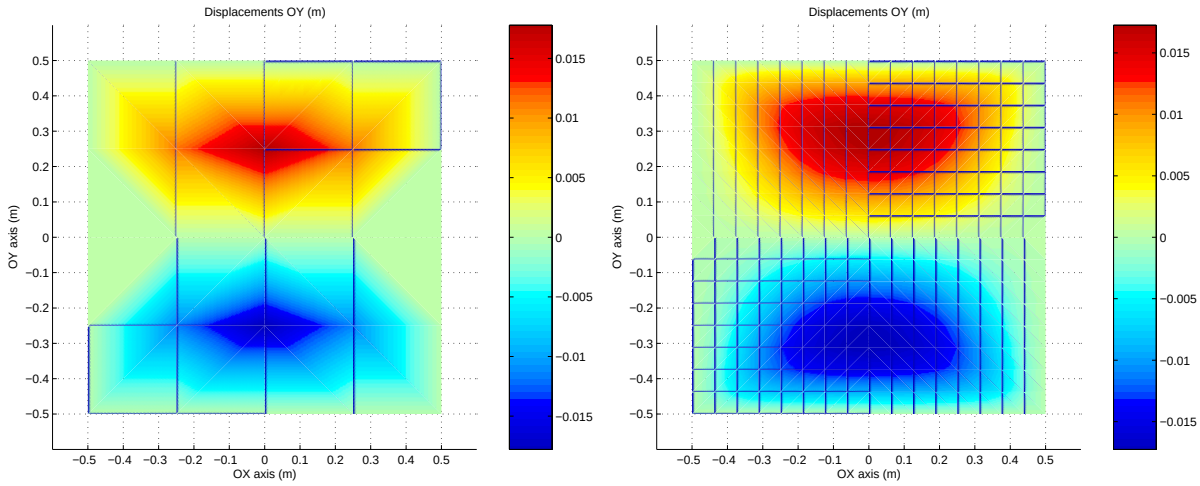

Figure 4.22: Example 4: Displacement in y-direction 1. Numerical 1, 2. Numerical 2

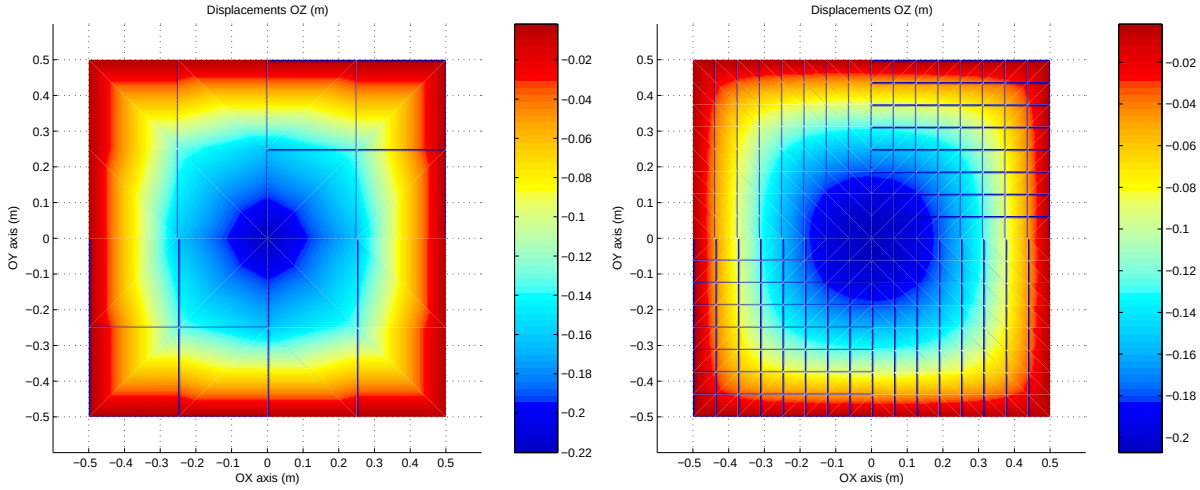

Figure 4.23: Example 4: Displacement in z-direction 1. Numerical 1, 2. Numerical 2

it is quadratic. This example shows the over all well implementation of the bending formulation.

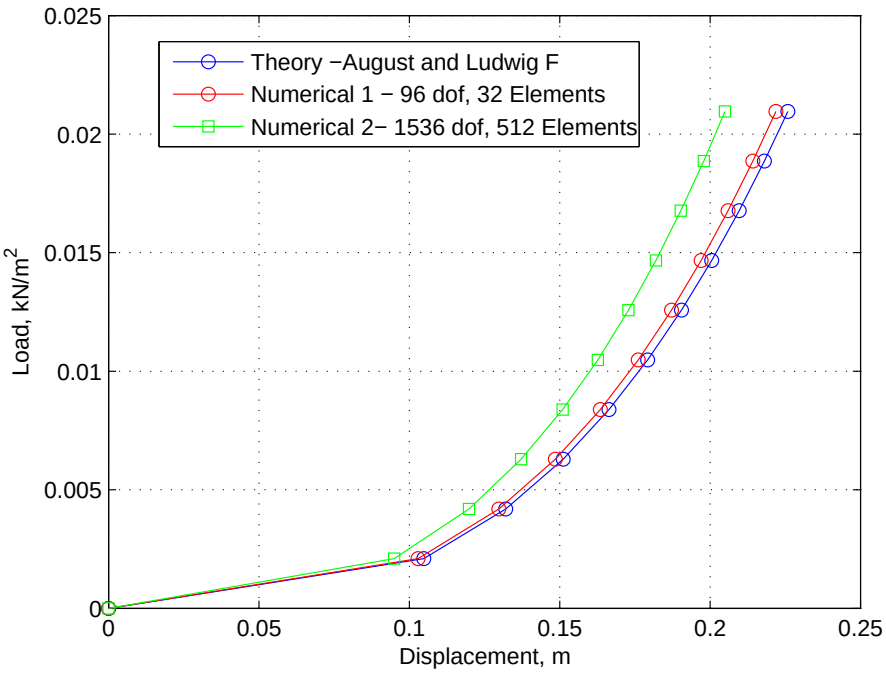

Figure 4.24: Example 4: Load - deflection curve for center of the membrane

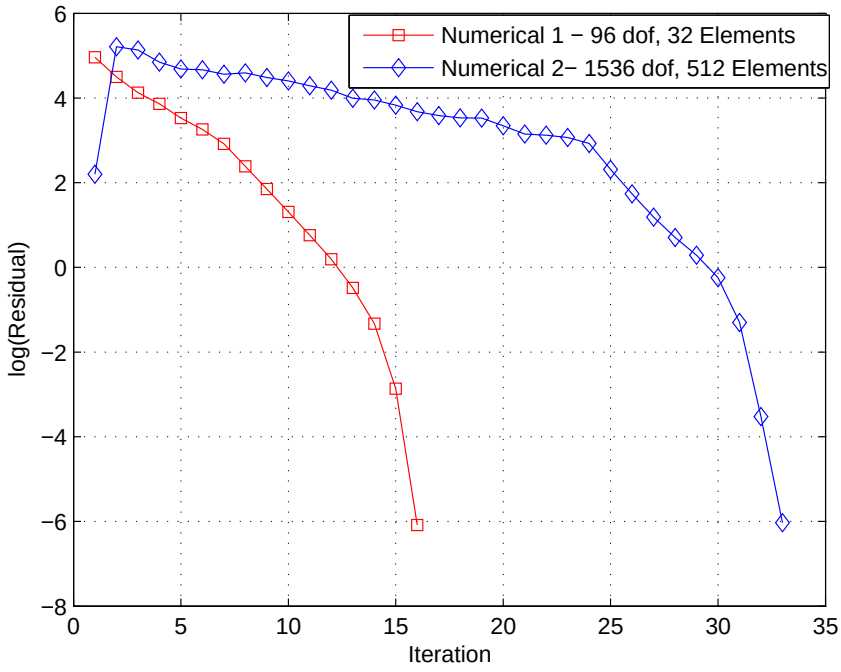

Figure 4.25: Example 4: Convergence curves

Chapter 5

Conclusion and Further Research

5.1 General considerations

The preceding chapters have presented the rotation free element for the analysis of membranes. These structures, comprised of cables and membranes, with broad application in Civil Engineering and Architecture, are subjected to large displacements and deformations, yet moderate strains.

A Total Lagrangian formulation for prestressed structural membranes was described. The kinematics of prestressed membranes was displayed as a series of three successive configurations, namely, a nominally stressed initial equilibrium state, a prestressed state and a final in-service state, for the time instants t^0, t^{pret} and t, respectively. Kinematic entities are fully derived, i.e., deformations gradient tensor, displacement gradient tensor, right Cauchy-Green tensor or Green-Lagrange strain tensor.The Saint Venant-Kirchhoff model is chosen as hyperelastic materials to describe moderate strains behavior.

The equilibrium shapes are employed as initial guesses for the subsequent highly nonlinear problem that entails the structural analysis of the membrane under the actual presence of prestressing loading and external loading.

A Total Lagrangian format set up along with a displacement-based isoparametric finite element formulation and a Newton-Raphson numerical scheme is adopted for the implementation of the rotation free elements. Two-noded and three-noded linear finite elements were employed to describe appropriately cable and membrane elements and for the bending formulation.

The set of equilibrium equations presented a geometrically nonlinear feature, so an iterative solution scheme was required. Among all the available methods, the second-

order Newton-Raphson technique accomplished the best convergence properties. The total tangent stiffness matrix required to be calculated by this method was obtained by linearizing the global equilibrium equations.

Apart from the well known second order Newton-Raphson method, other first order procedures such as the steepest descent method, the Polak-Ribiere method or the Fletcher-Reeves method are employed. This results in a very flexible numerical solver.

5.2 Conclusions

1. The pure membrane formulation shows instability problem especially for laterally loaded membranes. The bending formulation helps to solve such problems. Through series of example, the robustness and the validity of the rotation free formulation for membrane has been proven. The two example that has been shown, has a very close approximation to solution as reported in the literature.

2. The initial steps for a prestressing loading analysis are very unstable, specially when dealing with nearly plane initial membranes. The inclusion of a fictitious prestress to the total tangent stiffness matrix by the Levenberg-Marquardt method can be considered very useful.

3. Another appealing way to overcome difficulties throughout the first increments of the analysis is to combine first and second order methods in an efficient manner. To avoid initial divergences of the calculation, a more robust first order method is employed and only when local convergence is presumed,a second order algorithmic technique is used.

4. The Newton method has been proven as the most powerful method given its quadratic convergence. As a matter of fact, this method should be preferred, whether possible, over other techniques, such as dynamic relaxation, steepest descent or so on.

5.3 Recommendations for further research

The following are suggested for further development of the algorithm:

1. Incorporate a new constitutive model in the algorithm.

2. Introduce an optimization function into the algorithm which could optimize the membrane design in terms of cost, distribution of prestress, etc.

3. Modified the algorithm in order to simulate the interaction between fluid and structure.

4. Develop creeping modelling of membrane structures under different environment conditions.

5. More examples from the literature can run to further validate the formulation.

small

Bibliography

[1] August and ludwig Foppl. *Drang und Zwang*, volume vol 1. p.226, 1924. [cited at p. 50]

[2] W. K. Liu Belytschko T. and B. Moran. *Nonlinear finite elements for continua and structures*. John Wiley and Sons, 2000. [cited at p. 11, 14]

[3] J. Bonet and J. Mahaney. Form finding of membrane structures by the updated reference method with minimum mesh distortion. *International Journal of Solids and Structures 38, 5469-5480.*, 2001. [cited at p. 17, 36]

[4] J. Bonet, R. D. Wood, J. Mahaney, and P. Heywood. Finite element analysis of air supported membrane structures. *Computer methods in applied mechanics and engineering 190, 579-595*, 2000. [cited at p. 17, 36]

[5] Javier Bonet and Richard D. Wood. *Nonlinear Continuum Mechanics For Finite Element Analysis*. Cambridge University Press, 1997. [cited at p. 10, 19, 23, 40]

[6] Peter Broughton and Paul Ndumbaro. *Analysis of cable and Catenary Structures*. Thomas Telford, 1994. [cited at p. 7, 17, 36]

[7] Manfredo P. do Carmo. *Differential Geometry of Curves and Surfaces*. Pretice-Hall Inc, Englewood Cliff, New Jersey, 1976. [cited at p. 5, 7]

[8] Djordje Peric E A De Souza Net0 and D.R.J Owen. Finite elasticity in the spatial description: linearlization aspects with 3-d membrane applications. *Int. Jou. For Num. Meth. In Eng. Vol 38, 3365-3381*, 1995. [cited at p. 17, 36]

[9] E.Onate and M.Cervera. Derivation of thin plate bending elements with one degree of freedom per node. *Engrg. Comput. 10 553561.*, 1993. [cited at p. 7, 36]

[10] Michael Ortiz Fehmi Cirak and Peter Schroder. Subdivision surfaces: a new paradigm for thin-shell finite-element analysis. *Int. J. Numer. Meth. Engng. 47:2039-2072*, 2000. [cited at p. 36]

[11] A.J. Gil. *Structural Analysis of Prestressed Saint Venant-Kirchoff Hyperelastic membranes*. PhD thesis, Univeristy of Wales, Swansea, 2004. [cited at p. 7, 10, 36]

[12] A.J Gil and J Bonet. Finite element analysis of prestressed structural membrane. *Finite Element in Analysis and Design 42 683-697*, 2006. [cited at p. 36]

[13] A.J Gil and J Bonet. Structural analysis of prestressed saint venant-kirchhoff hyperelastic membrane subjected to moderate strains. *Computer and Structutes 84 1012-1028*, 2006. [cited at p. 17, 36]

[14] Chan HC Hampshire JK, Topping BHV. Three node triangular elements with one degree of freedom per node. *Engineering Computations 9: 49-62*, 1992. [cited at p. 7, 36]

[15] Gerhard A. Holzapfel. *Nonlinear Solid Mechanics: A Continuum Approach for Engineering*. John Wiley and Sons Ltd, 2001. [cited at p. 10, 11]

[16] Max Irvine. *Cables Structures*. Dover Publication, Inc.,New York, 1992. [cited at p. 7, 17, 36]

[17] Kai-Uwe Bletzinger Johannes Linhard, Roland Wuchner. Upgrading membranes to shells- the ceg rotation free shell element and its application in structural analysis. *Finite Elements in Analysis and Design 44 63 74*, 2007. [cited at p. 7, 36]

[18] Bathe K. *Finite element procedures*. New Jersey: Prentice-Hall, Inc., 1996. [cited at p. 14]

[19] Robert Levy and William R.Spillers. *Analysis of Geometrically Nonlinear Structures*. Chapman and Hall, 1995. [cited at p. 6, 7]

[20] Klaus Linkwitz. About formfinding of double-curved structures. *Engineering Structures 21 709718*, 1999. [cited at p. 7, 28]

[21] Lawrence E. Malvern. *introduction to the Mechanics of a Continuum Medium*. Pretice-Hall Inc, Englewood Cliff, New Jersey, 1969. [cited at p. 11]

[22] Barnes MR. Form finding and analysis of tension space structure by dynamic relaxation. *PhD Thesis, Department of Civil Engineering, The City University, London*, 1977. [cited at p. 7]

[23] A Nadai. *Elastische Platten*. page 288, 1925. [cited at p. 49, 50]

[24] Zienkiewicz O.C. and Taylor R.L. *Finite Element Method*. Fifth edition,Butterworth-Heinemann, 2000. [cited at p. 14]

[25] F. Otto. *Tensile Structures*. M.I.T Press, Cambridge, 1973. [cited at p. 17, 36]

[26] Phaal and C.R. Calladine. A simple class of finite elements for plate and shell problems. ii: an element for thin shells with only translational degrees of freedom. *Int. J. Numer. Methods Engrg. 35 979996*, 1992. [cited at p. 7, 36]

[27] Nay RA and Utku S. An alternative to the finite element method. *Variational Methods Engineering 1*, 1972. [cited at p. 7, 36]

[28] BRITISH STANDARD. Loading for buildings. *BS 6399 : Part 3*, 1988. [cited at p. 30]

[29] Timoshenko and Woinowsky-Krieger. *Theory of plates and Shells*. McGraw-Hill book company, second edition, 1959. [cited at p. 6, 17, 36, 49, 50]

[30] Oren Vilnay. *Cable Nets and Tensegric shells*. Pretice-Hall Inc, Englewood Cliff, New Jersey, 1990. [cited at p. 7, 17, 36]

[31] D.S. Wakefield. Engineering analysis of tension structures: Theory and practice. *Engineering Structures 21 680-690*, 1999. [cited at p. 2]

[32] John william Leonard. *Tension Structures - Behavior and Analysis*. McGraw-Hill Book Company, 1988. [cited at p. 2, 6, 7, 17, 36]